

Variational Bayesian inference for CP tensor completion with side information

Stanislav Budzinskiy¹ and Nikolai Zamarashkin¹

¹Marchuk Institute of Numerical Mathematics RAS

Abstract

We propose a message passing algorithm, based on variational Bayesian inference, for low-rank tensor completion with automatic rank determination in the canonical polyadic format when additional side information (SI) is given. The SI comes in the form of low-dimensional subspaces the contain the fiber spans of the tensor (columns, rows, tubes, etc.). We validate the regularization properties induced by SI with extensive numerical experiments on synthetic and real-world data and present the results about tensor recovery and rank determination. The results show that the number of samples required for successful completion is significantly reduced in the presence of SI. We also discuss the origin of a bump in the phase transition curves that exists when the dimensionality of SI is comparable with that of the tensor.

Contents

1	Introduction	3
2	Notation	4
3	Matrix completion with side information	5
3.1	Probabilistic model: priors	5
3.2	Variational Bayesian inference	6
3.3	Optimal posterior distributions	7
3.3.1	Factor matrices U and V	7
3.3.2	Precision matrix Λ	8
3.3.3	Noise precision τ	8
3.4	Message passing updates	8
4	Tensor completion with side information	9
4.1	Probabilistic model: priors	9
4.2	Optimal posterior distributions	10
4.2.1	Canonical factors U_l	10
4.2.2	Precision matrix Λ	11
4.2.3	Noise precision τ	11
4.3	Message passing updates	11

5	Numerical experiments	12
5.1	Computational complexity	12
5.2	Initialization	13
5.3	Synthetic data	13
5.3.1	Performance of completion	13
5.3.2	Performance of rank determination	15
5.4	Facial images	16
6	Discussion	19
A	Used distributions	26
B	Optimal factorized variational distributions	26
B.1	General form	26
B.2	Matrix case	27
B.2.1	Factor matrices U and V	27
B.2.2	Precision matrix Λ	29
B.2.3	Noise precision τ	29
B.3	Tensor case	29
B.3.1	Canonical factors U_l	29
B.3.2	Precision matrix Λ	31
B.3.3	Noise precision τ	31
B.4	Computing the expectations	31
C	Distribution of predicted values	32
D	Additional numerical experiments with synthetic data	33

1 Introduction

A big part of modern signal processing is based on working with multi-dimensional signals that exhibit some kind of hidden structure: this typically means sparsity in a certain basis/frame or low-rankedness. One of the principal ideas is to leverage the signal's structure to reconstruct it from a series of measurements that can be, on the one hand, scant and, on the other hand, corrupted by noise and outliers. The advent of computationally feasible algorithms for compressed sensing [1], matrix completion [2, 3], and robust principal component analysis [4] marked the beginning of a new era in signal processing.

In certain applications, knowing that the signal is structured is not the only piece of information we have at our disposal. Some auxiliary information might be available as well, which can come in a variety of different forms: as an approximate solution to the problem [5, 6]; as a graph describing the relations between the elements of the data [7, 8]; as an accompanying dataset that shares some of the latent factors [9, 10]; as low-dimensional subspaces containing row and column spans [11–15]. By incorporating auxiliary information in an algorithm, we aim to help it recover signals using fewer measurements and in the presence of more severe corruption. The possible applications of auxiliary information include, for example, recommender systems [16], video processing [17], and bioinformatics [18–20]. In what follows, we fix the name *side information* for the auxiliary information in the form of low-dimensional subspaces.

Our focus is on tensor completion, or tensor factorization from incomplete data: given a multi-dimensional tensor, we want to reconstruct it from a small fraction of its elements. The problem is obviously ill-posed unless the tensor in question can be described with a small number of parameters and unless it is incoherent vis-à-vis the point measurements. For tensors, there exist several widely used low-parametric representations: the canonical polyadic (CP) decomposition (also known as CANDECOMP/PARAFAC), the Tucker decomposition, and the tensor train (TT) decomposition. See [21, 22] for an introduction to these tensor representations and [23–25] for a review of their applications.

The properties of Tucker and TT decompositions are closely related to those of low-rank matrix decompositions, which stems from the fact that Tucker and TT ranks are simply the ranks of certain tensor unfoldings or flattenings. This explains why similar techniques have been applied to solve low-rank matrix, Tucker, and TT completion problems: convex optimization based on nuclear norm minimization [2, 3, 26–28]; non-convex optimization approaches that minimize the residual based on low-rank projections [11, 29–31] or explicit factorization [32–38], including their Riemannian variants [39–44].

CP decomposition inherits less from the matrix case; for instance, the best low-rank approximation problem becomes ill-posed [45]. Consequently, CP completion is carried out by updating the canonical factors in an alternating fashion [46–48], and the canonical rank of the data is typically determined by explicitly fitting several CP models of different ranks.

An important group of methods we have not mentioned yet are probabilistic ones that employ the Bayesian inference machinery to solve matrix and tensor completion problems. The general approach consists in setting up a probabilistic model for the data and estimating its parameters and hyperparameters. In the seminal paper [49], a maximum a posteriori estimate was found for the latent factors of a low-rank matrix and it was noted that a fully Bayesian approach would give higher predictive accuracy. Computing the exact posterior distribution of the parameters conditioned on the data is typically impossible, so one has to adopt an approximate Bayesian inference strategy. The two dominant ones are Markov chain Monte Carlo (MCMC) sampling [50] and variational inference [51, 52], and both of them have been applied to matrix completion problems; see [53, 54] and [55–57], respectively.

Tensor completion has also been addressed with probabilistic and Bayesian methods for

Tucker [58, 59], TT [60], and CP [61–64] decompositions. The Bayesian framework is especially promising for CP factorization since inference of a probabilistic model based on Gaussian-Gamma priors achieves automatic rank determination [62]. These priors were first introduced for matrix completion [56] and have recently been extended to generalized hyperbolic priors [64]; other choices are possible too [54, 65].

In this article, we deal with what lies at the intersection of the topics mentioned above: Bayesian CP completion in the presence of side information. In fact, this amounts to finding a CP factorization of a Tucker core when the corresponding Tucker factors are known. Completion and factorization problems with different kinds of auxiliary information have been studied in the literature for CP [66–73] and Tucker [74] decompositions. Side information, as we defined it, received less attention: it was used for TT completion [75, 76], Tucker completion [77], and we have not seen such papers for the CP decomposition. Similar formulations appear in kernelized matrix completion [78, 79].

Our goal is to develop a tensor completion method for the CP decomposition using variational Bayesian inference and incorporating side information. To our knowledge, this is the first time side information is incorporated in CP tensor completion.

The paper begins with the matrix case: in Section 3 we formulate a probabilistic model, introduce the variational Bayesian approach, and present formulas for an iterative message passing inference algorithm. In Section 4 we turn to tensors and describe the corresponding CP completion approach. Section 5 is devoted to numerical experiments that give insight into the regularization properties of side information. All the details of the derivations can be found in the Appendix.

2 Notation

Matrices are denoted by uppercase letters (e.g. X), and we use bold uppercase letters (e.g. \mathbf{X}) for tensors. For a d -dimensional tensor \mathbf{X} of size $n_1 \times \dots \times n_d$, we write its element in position $(i_1, \dots, i_d) \in [n_1] \times \dots \times [n_d]$ as $x_{i_1 \dots i_d}$, where $[n] = \{1, \dots, n\}$. If a tensor \mathbf{X} admits a rank- r canonical decomposition with factor matrices $\{A_l\}$ of sizes $n_l \times r$, we can write it as

$$x_{i_1 \dots i_d} = \sum_{j=1}^r a_{1, i_1 j} \dots a_{d, i_d j}, \quad \mathbf{X} = \llbracket A_1, \dots, A_d \rrbracket.$$

The trace of a matrix is denoted by Tr . For a matrix X of size $mk \times nk$, we denote its j -th diagonal $m \times n$ block by $\text{block}_j X$. For a subset of indices $\Omega \subseteq [n_1] \times \dots \times [n_d]$ product and sum over Ω will be denoted by \prod_{Ω} and \sum_{Ω} , respectively.

The Kronecker and Hadamard (elementwise) products of matrices are denoted by \otimes and \odot , respectively. For d matrices $\{X_l\}$ of size $m \times n$, we define their multi-linear product as

$$\langle X_1, \dots, X_d \rangle = \sum_{i=1}^m \sum_{j=1}^n x_{1, ij} \dots x_{d, ij}.$$

This is a generalization of the Frobenius inner product

$$\langle X_1, X_2 \rangle_F = \text{Tr}\{X_1^T X_2\}, \quad \|X\|_F = \sqrt{\langle X, X \rangle_F}.$$

The Gaussian, Gamma, and Student’s distributions are written as \mathcal{N} , \mathcal{G} , and St , respectively. The expectation of a random variable is denoted by \mathbb{E} .

3 Matrix completion with side information

3.1 Probabilistic model: priors

Let $X \in \mathbb{R}^{n_1 \times n_2}$ be a rank- r matrix and $Y = X + E$ be the same matrix but corrupted by i.i.d. random Gaussian noise

$$p(E) = \prod_{i_1=1}^{n_1} \prod_{i_2=1}^{n_2} \mathcal{N}(\varepsilon_{i_1 i_2} | 0, \tau^{-1})$$

with zero mean and precision $\tau > 0$. In matrix completion we have access only to those entries of Y that belong to a given collection of indices $\Omega \subseteq [n_1] \times [n_2]$:

$$Y_\Omega = \mathcal{P}_\Omega(X + E) \in \mathbb{R}^{n_1 \times n_2}.$$

The operator $\mathcal{P}_\Omega : \mathbb{R}^{n_1 \times n_2} \rightarrow \mathbb{R}^{n_1 \times n_2}$ keeps intact the elements of a matrix that lie in Ω and sets to zero all the remaining ones.

In the setting of completion with side information, we are additionally given a pair of subspaces spanned by the columns of full-rank matrices

$$G = \begin{bmatrix} g_1^T \\ g_2^T \\ \vdots \\ g_{n_1}^T \end{bmatrix} \in \mathbb{R}^{n_1 \times m_1}, \quad H = \begin{bmatrix} h_1^T \\ h_2^T \\ \vdots \\ h_{n_2}^T \end{bmatrix} \in \mathbb{R}^{n_2 \times m_2}$$

with $m_1 < n_1$ and $m_2 < n_2$ and it is known that these subspaces contain the column and row spaces of X , respectively:

$$\text{col}X \subseteq \text{col}G, \quad \text{col}X^T \subseteq \text{col}H.$$

We can express the a priori information about X in a compact form by writing it as a product $X = GU(HV)^T$, where

$$U = \begin{bmatrix} u_1^T \\ u_2^T \\ \vdots \\ u_{m_1}^T \end{bmatrix} \in \mathbb{R}^{m_1 \times k}, \quad V = \begin{bmatrix} v_1^T \\ v_2^T \\ \vdots \\ v_{m_2}^T \end{bmatrix} \in \mathbb{R}^{m_2 \times k}$$

are the unknown factors that we need to recover; $k \geq r$ serves as a possibly overestimated prediction of the rank. As a result, the conditional distribution of Y_Ω becomes

$$p(Y_\Omega | U, V, \tau) = \prod_{\Omega} \mathcal{N}(y_{i_1 i_2} | g_{i_1}^T U V^T h_{i_2}, \tau^{-1}).$$

Note that this model is different from [13], where the interaction between G and U , and between H and V , is subject to Gaussian noise.

Following [56], assume that the rows of U and V are i.i.d. random Gaussian vectors

$$p(U | \Lambda) = \prod_{i_1=1}^{n_1} \mathcal{N}(u_{i_1} | 0, \Lambda^{-1}),$$

$$p(V | \Lambda) = \prod_{i_2=1}^{n_2} \mathcal{N}(v_{i_2} | 0, \Lambda^{-1}),$$

with zero mean and precision matrix $\Lambda = \text{diag}(\lambda_j) \in \mathbb{R}^{k \times k}$. The idea behind this prior is twofold. First, it enforces the columns of U and V to be balanced in terms of their norms. Second, if some of the λ_j are large, the corresponding columns of U and V have little impact and can be removed to reduce the rank prediction k . We fix a Gamma hyperprior, parametrized with shape and rate parameters, for the precision matrix:

$$p(\Lambda) = \prod_{j=1}^k \mathcal{G}(\lambda_j | a_j, b_j).$$

Gaussian random variables with Gamma-distributed precision are ubiquitous in Bayesian inference since they form an exponentially conjugate pair (see Appendix). Finally, we choose a Gamma hyperprior for the noise precision as well,

$$p(\tau) = \mathcal{G}(\tau | a_0, b_0),$$

which gives us the following joint distribution:

$$p(Y_\Omega, U, V, \Lambda, \tau) = p(Y_\Omega | U, V, \tau) p(U | \Lambda) p(V | \Lambda) p(\Lambda) p(\tau).$$

3.2 Variational Bayesian inference

We now turn to the posterior distribution of the model parameters conditioned on the observed data:

$$p(U, V, \Lambda, \tau | Y_\Omega) = \frac{p(Y_\Omega, U, V, \Lambda, \tau)}{\int p(Y_\Omega, U, V, \Lambda, \tau) dU dV d\Lambda d\tau}.$$

Exact Bayesian inference consists in evaluating $p(U, V, \Lambda, \tau | Y_\Omega)$, which, however, is not an option, since the evidence of the model, the denominator of the right hand side, is an intractable integral. So approximate inference methods need to be used that seek a distribution $q(U, V, \Lambda, \tau)$ such that

$$q(U, V, \Lambda, \tau) \approx p(U, V, \Lambda, \tau | Y_\Omega).$$

To this end, we use variational Bayesian inference.

Denote by $\Theta = (\theta_1, \theta_2, \theta_3, \theta_4) = (U, V, \Lambda, \tau)$ the model parameters. We will look for a factorized variational distribution

$$q(\Theta) = q(U)q(V)q(\Lambda)q(\tau)$$

that minimizes the Kullback–Leibler divergence

$$\mathcal{KL}[q(\Theta) || p(\Theta | Y_\Omega)] = \int q(\Theta) \log \frac{q(\Theta)}{p(\Theta | Y_\Omega)} d\Theta.$$

Simple algebra shows that this is equivalent to minimizing

$$\int q(\Theta) \log \frac{q(\Theta)}{p(Y_\Omega, \Theta)} d\Theta \rightarrow \min_{q(\Theta)}.$$

If we now substitute the factorized form of $q(\Theta)$ and attempt to minimize over $q(\theta_i)$ with all the remaining $q(\theta_j)$, $j \neq i$, fixed, we will see that the minimum is attained at the optimal distribution $q^*(\theta_i)$, whose logarithm is

$$\log q^*(\theta_i) = \mathbb{E}_{\sim \theta_i} \{\log p(Y_\Omega, \Theta)\} + \text{const.}$$

The notation $\mathbb{E}_{\sim\theta_i}$ stands for the expectation with respect to the distribution $\prod_{j \neq i} q(\theta_j)$, and the constant contains the logarithm of the normalization factor. This gives rise to a message-passing algorithm for variational Bayesian inference, where we update the distributions iteratively for each θ_i one by one and which converges to a local minimum [52].

What is particularly appealing in the variational Bayesian inference approach for our model is that the optimal distributions $q^*(\theta_i)$ are of the same form as the corresponding prior distributions, owing to the exponential conjugacy. Below, we present the explicit formulas for the $q^*(\theta_i)$. Find their derivations in the Appendix.

3.3 Optimal posterior distributions

3.3.1 Factor matrices U and V

Denote by $\bar{u} \in \mathbb{R}^{m_1 k}$ and $\bar{v} \in \mathbb{R}^{m_2 k}$ the vectorizations of U and V obtained by stacking their columns as

$$\begin{aligned}\bar{u} &= [u_{11} \quad \dots \quad u_{m_1 1} \quad u_{12} \quad \dots \quad u_{m_1 k}]^T, \\ \bar{v} &= [v_{11} \quad \dots \quad v_{m_2 1} \quad v_{12} \quad \dots \quad v_{m_2 k}]^T,\end{aligned}$$

and let \mathbb{E} with no subscript be the expectation with respect to the product of those $q(\theta_i)$, for which θ_i is included in the expression that is averaged.

The optimal posterior distribution for the factor matrix U is a Gaussian distribution of its vectorization

$$q^*(U) = \mathcal{N}(\bar{u} | \mu_{\bar{u}}, A_{\bar{u}})$$

with covariance

$$\begin{aligned}A_{\bar{u}} &= \left[\mathbb{E}\{\Lambda\} \otimes I_{m_1} + \mathbb{E}\{\tau\} B_{\bar{u}} \right]^{-1}, \\ B_{\bar{u}} &= \sum_{\Omega} (I_k \otimes h_{i_2}^T) \mathbb{E}\{\bar{v}\bar{v}^T\} (I_k \otimes h_{i_2}) \otimes g_{i_1} g_{i_1}^T\end{aligned}$$

and mean

$$\mu_{\bar{u}} = \mathbb{E}\{\tau\} A_{\bar{u}} \sum_{\Omega} y_{i_1 i_2} (I_k \otimes h_{i_2}^T) \mathbb{E}\{\bar{v}\} \otimes g_{i_1}.$$

If the side information is trivial, that is G and H are square identity matrices, we recognize block-diagonal structure in $A_{\bar{u}}$, and the rows of U remain independent in the posterior just as in the prior (cf. [56]). The non-trivial side information, on the contrary, intertwines the rows; if, however, the side information is incorporated as in [13], the rows stay independent.

Similarly

$$q^*(V) = \mathcal{N}(\bar{v} | \mu_{\bar{v}}, A_{\bar{v}})$$

with

$$\begin{aligned}A_{\bar{v}} &= \left[\mathbb{E}\{\Lambda\} \otimes I_{m_2} + \mathbb{E}\{\tau\} B_{\bar{v}} \right]^{-1}, \\ B_{\bar{v}} &= \sum_{\Omega} (I_k \otimes g_{i_1}^T) \mathbb{E}\{\bar{u}\bar{u}^T\} (I_k \otimes g_{i_1}) \otimes h_{i_2} h_{i_2}^T\end{aligned}$$

and

$$\mu_{\bar{v}} = \mathbb{E}\{\tau\} A_{\bar{v}} \sum_{\Omega} y_{i_1 i_2} (I_k \otimes g_{i_1}^T) \mathbb{E}\{\bar{u}\} \otimes h_{i_2}.$$

3.3.2 Precision matrix Λ

The optimal posterior distribution for the precision matrix Λ of the factors U and V is again a product of Gamma distributions

$$q^*(\Lambda) = \prod_{j=1}^k \mathcal{G}(\lambda_j | c_j, d_j)$$

but with shifted shape and rate parameters for $j = 1, \dots, k$:

$$c_j = a_j + \frac{m_1 + m_2}{2}, \quad d_j = b_j + \frac{1}{2} \mathbb{E}\{U^T U\}_{jj} + \frac{1}{2} \mathbb{E}\{V^T V\}_{jj}.$$

For instance, the parameters of the posterior distribution depend on the side information only via the dimensions of the subspaces and not the subspaces themselves.

3.3.3 Noise precision τ

The optimal posterior distribution for the noise precision τ follows a Gamma distribution

$$q^*(\tau) = \mathcal{G}(\tau | c_0, d_0)$$

with

$$c_0 = a_0 + \frac{|\Omega|}{2}, \quad d_0 = b_0 + \frac{1}{2} \mathbb{E}\left\{\|Y_\Omega - \mathcal{P}_\Omega(GUV^T H^T)\|_F^2\right\}.$$

The rate parameter is updated by the averaged squared Frobenius norm of the residual.

3.4 Message passing updates

To turn the expressions for the optimal distributions $q^*(\theta_i)$ into an iterative algorithm, it remains to explicitly compute the expectations. An iteration of the message passing algorithm then proceeds as follows. At first, we update the covariance for the matrix factor U :

$$\begin{aligned} B_{\bar{u}} &\leftarrow \sum_{\Omega} (I_k \otimes h_{i_2}^T) (\mu_{\bar{v}} \mu_{\bar{v}}^T + A_{\bar{v}}) (I_k \otimes h_{i_2}) \otimes g_{i_1} g_{i_1}^T, \\ A_{\bar{u}} &\leftarrow \left[\text{diag} \left(\frac{c_j}{d_j} \right) \otimes I_{m_1} + \frac{c_0}{d_0} B_{\bar{u}} \right]^{-1}. \end{aligned} \tag{1}$$

This new $A_{\bar{u}}$ is used to calculate the corresponding mean:

$$\mu_{\bar{u}} \leftarrow \frac{c_0}{d_0} A_{\bar{u}} \sum_{\Omega} y_{i_1 i_2} (I_k \otimes h_{i_2}^T) \mu_{\bar{v}} \otimes g_{i_1}. \tag{2}$$

Then, in a similar fashion, we evaluate the new covariance

$$\begin{aligned} B_{\bar{v}} &\leftarrow \sum_{\Omega} (I_k \otimes g_{i_1}^T) (\mu_{\bar{u}} \mu_{\bar{u}}^T + A_{\bar{u}}) (I_k \otimes g_{i_1}) \otimes h_{i_2} h_{i_2}^T, \\ A_{\bar{v}} &\leftarrow \left[\text{diag} \left(\frac{c_j}{d_j} \right) \otimes I_{m_2} + \frac{c_0}{d_0} B_{\bar{v}} \right]^{-1} \end{aligned} \tag{3}$$

and mean

$$\mu_{\bar{v}} \leftarrow \frac{c_0}{d_0} A_{\bar{v}} \sum_{\Omega} y_{i_1 i_2} (I_k \otimes g_{i_1}^T) \mu_{\bar{u}} \otimes h_{i_2} \tag{4}$$

for the second factor matrix V . The shape parameters of $q^*(\Lambda)$ are updated once and for all as

$$c_j \leftarrow a_j + \frac{m_1 + m_2}{2}, \quad j = 1, \dots, k, \quad (5)$$

while the rate parameters are recomputed on each iteration of the message passing procedure:

$$\begin{aligned} d_j \leftarrow b_j + \frac{1}{2} \text{Tr} \{ \text{block}_j(\mu_{\bar{u}} \mu_{\bar{u}}^T + A_{\bar{u}}) \} \\ + \frac{1}{2} \text{Tr} \{ \text{block}_j(\mu_{\bar{v}} \mu_{\bar{v}}^T + A_{\bar{v}}) \}, \quad j = 1, \dots, k, \end{aligned} \quad (6)$$

where $\text{block}_j A_{\bar{u}} \in \mathbb{R}^{m_1 \times m_1}$ is the j -th diagonal block of $A_{\bar{u}}$. Likewise, the shape hyperparameter for noise precision is set only once

$$c_0 \leftarrow a_0 + \frac{|\Omega|}{2}, \quad (7)$$

but the corresponding rate parameter is evaluated every time:

$$\begin{aligned} d_0 \leftarrow b_0 + \frac{1}{2} \sum_{\Omega} \left[(y_{i_1 i_2} - g_{i_1}^T M_{\bar{u}} M_{\bar{v}}^T h_{i_2})^2 \right. \\ + g_{i_1}^T M_{\bar{u}} (I_k \otimes h_{i_2}^T) A_{\bar{v}} (I_k \otimes h_{i_2}) M_{\bar{u}}^T g_{i_1} \\ + h_{i_2}^T M_{\bar{v}} (I_k \otimes g_{i_1}^T) A_{\bar{u}} (I_k \otimes g_{i_1}) M_{\bar{v}}^T h_{i_2} \\ \left. + \text{Tr} \{ A_{\bar{v}} (I_k \otimes h_{i_2} g_{i_1}^T) A_{\bar{u}} (I_k \otimes g_{i_1} h_{i_2}^T) \} \right], \end{aligned} \quad (8)$$

where we denote by $M_{\bar{u}} \in \mathbb{R}^{m_1 \times k}$ and $M_{\bar{v}} \in \mathbb{R}^{m_2 \times k}$ the matricizations of $\mu_{\bar{u}}$ and $\mu_{\bar{v}}$, respectively.

Having computed the new posterior distribution $q(\Theta)$, we can reduce the rank prediction k by removing those columns of U and V , for which the mean c_j/d_j of $q(\lambda_j)$ is large.

We can also approximately compute the distribution of the unknown elements of Y . Namely, for $(i_1, i_2) \notin \Omega$ the distribution of $y_{i_1 i_2}$ conditioned on Y_{Ω} is close to a Student's t -distribution

$$p(y_{i_1 i_2} | Y_{\Omega}) \approx \text{St} (y_{i_1 i_2} | g_{i_1}^T M_{\bar{u}} M_{\bar{v}}^T h_{i_2}, \xi, 2c_0)$$

with

$$\begin{aligned} \xi = \left[\frac{d_0}{c_0} + h_{i_2}^T M_{\bar{v}} (I_k \otimes g_{i_1}^T) A_{\bar{u}} (I_k \otimes g_{i_1}) M_{\bar{v}} h_{i_2} \right. \\ \left. + g_{i_1}^T M_{\bar{u}} (I_k \otimes h_{i_2}^T) A_{\bar{v}} (I_k \otimes h_{i_2}) M_{\bar{u}}^T h_{i_2} \right]^{-1}. \end{aligned}$$

So its mean is $g_{i_1}^T M_{\bar{u}} M_{\bar{v}}^T h_{i_2}$ and its variance is $\frac{c_0}{\xi(c_0 - 1)}$.

4 Tensor completion with side information

4.1 Probabilistic model: priors

Let $\mathbf{X} \in \mathbb{R}^{n_1 \times \dots \times n_d}$ be a d -dimensional tensor with canonical rank equal to r . Assume that for every dimension we have full-rank side information matrices

$$G_l = \begin{bmatrix} g_{l,1}^T \\ g_{l,2}^T \\ \vdots \\ g_{l,n_l}^T \end{bmatrix} \in \mathbb{R}^{n_l \times m_l}, \quad l = 1, \dots, d.$$

If $k \geq r$ is our prediction of the canonical rank, the latent factor matrices of the canonical decomposition are

$$U_l = \begin{bmatrix} u_{l,1}^T \\ u_{l,2}^T \\ \vdots \\ u_{l,n_l}^T \end{bmatrix} \in \mathbb{R}^{m_l \times k}, \quad l = 1, \dots, d.$$

This allows us to write every element of the tensor \mathbf{X} as a multi-linear product of length- k vectors

$$x_{i_1 \dots i_d} = \langle U_1^T g_{1,i_1}, \dots, U_d^T g_{d,i_d} \rangle = \sum_{j=1}^k (U_1^T g_{1,i_1})_j \dots (U_d^T g_{d,i_d})_j.$$

As a shorthand for this, we will write $\mathbf{X} = \llbracket G_1 U_1, \dots, G_d U_d \rrbracket$. Just as in the two-dimensional matrix case, we have access only to a subset of entries that are additionally corrupted by noise. Denote by $\Omega \subseteq [n_1] \times \dots \times [n_d]$ the corresponding collection of multi-indices and let $\mathbf{E} \in \mathbb{R}^{n_1 \times \dots \times n_d}$ be a tensor with i.i.d random Gaussian components

$$p(\mathbf{E}) = \prod_{i_1=1}^{n_1} \dots \prod_{i_d=1}^{n_d} \mathcal{N}(\varepsilon_{i_1 \dots i_d} | 0, \tau^{-1}).$$

Then what we know is a sample $\mathbf{Y}_\Omega = \mathcal{P}_\Omega(\mathbf{X} + \mathbf{E})$ that is distributed according to

$$p(\mathbf{Y}_\Omega | U_1, \dots, U_d, \tau) = \prod_{\Omega} \mathcal{N}(y_{i_1 \dots i_d} | \langle U_1^T g_{1,i_1}, \dots, U_d^T g_{d,i_d} \rangle, \tau^{-1}).$$

We choose the same priors as before for the factor matrices

$$p(U_l | \Lambda) = \prod_{i_l=1}^{n_l} \mathcal{N}(u_{l,i_l} | 0, \Lambda^{-1}), \quad l = 1, \dots, d,$$

and the hyperparameters

$$p(\Lambda) = \prod_{j=1}^k \mathcal{G}(\lambda_j | a_j, b_j), \quad p(\tau) = \mathcal{G}(\tau | a_0, b_0).$$

4.2 Optimal posterior distributions

The variational inference framework with a factorized distribution $q(\Theta)$ can be applied in the tensor case too. It provides optimal posterior distributions $q^*(\theta_i)$ that, due to exponential conjugacy, are of the same form as the corresponding priors.

4.2.1 Canonical factors U_l

The optimal posterior distribution for each canonical factor U_l is a Gaussian distribution of its vectorization

$$q^*(U_l) = \mathcal{N}(\bar{u}_l | \mu_l, A_l).$$

To present the formulas for the mean and covariance, it is convenient to express multi-linear products in terms of the Hadamard product. For every $l = 1, \dots, d$ we have

$$\langle U_1^T g_{1,i_1}, \dots, U_d^T g_{d,i_d} \rangle = (U_l^T g_{l,i_l})^T \bigodot_{s \neq l} U_s^T g_{s,i_s}.$$

Then the covariance matrix $A_l \in \mathbb{R}^{m_l k \times m_l k}$ can be written as

$$A_l = \left[\mathbb{E}\{\Lambda\} \otimes I_{m_l} + \mathbb{E}\{\tau\} B_l \right]^{-1},$$

$$B_l = \sum_{\Omega} \left(\bigodot_{s \neq l} (I_k \otimes g_{s,i_s}^T) \mathbb{E}\{\bar{u}_s \bar{u}_s^T\} (I_k \otimes g_{s,i_s}) \right) \otimes g_{l,i_l} g_{l,i_l}^T,$$

and the mean is

$$\mu_l = \mathbb{E}\{\tau\} A_l \sum_{\Omega} y_{i_1 \dots i_d} \left(\bigodot_{s \neq l} \mathbb{E}\{U_s^T\} g_{s,i_s} \right) \otimes g_{l,i_l}.$$

4.2.2 Precision matrix Λ

As previously, the components of the diagonal precision matrix Λ are independent Gamma random variables in the posterior distribution:

$$q^*(\Lambda) = \prod_{j=1}^k \mathcal{G}(\lambda_j | c_j, d_j).$$

The formulas for their parameters are simple multi-dimensional extensions of what we saw in the matrix case, that is for $j = 1, \dots, k$ we have

$$c_j = a_j + \frac{1}{2} \sum_{l=1}^d m_l, \quad d_j = b_j + \frac{1}{2} \sum_{l=1}^d \mathbb{E}\{U_l^T U_l\}_{jj}.$$

4.2.3 Noise precision τ

As for the precision parameter τ of the noise, it follows a posterior Gamma distribution

$$q^*(\tau) = \mathcal{G}(\tau | c_0, d_0)$$

with shape and rate given by

$$c_0 = a_0 + \frac{|\Omega|}{2}, \quad d_0 = b_0 + \frac{1}{2} \mathbb{E}\left\{ \|\mathbf{Y}_{\Omega} - \mathcal{P}_{\Omega}[\![G_1 U_1, \dots, G_d U_d]\!]\|_F^2 \right\}.$$

4.3 Message passing updates

It is now straightforward to turn the formulas for the optimal posterior distributions into a message passing algorithm. On each iteration, we will start by updating the posteriors of the canonical factors one by one: the covariance

$$B_l \leftarrow \sum_{\Omega} \left(\bigodot_{s \neq l} \left[(I_k \otimes g_{s,i_s}^T) A_s (I_k \otimes g_{s,i_s}) + M_s^T g_{s,i_s} g_{s,i_s}^T M_s \right] \right) \otimes g_{l,i_l} g_{l,i_l}^T, \quad (9)$$

$$A_l \leftarrow \left[\text{diag} \left(\frac{c_j}{d_j} \right) \otimes I_{m_l} + \frac{c_0}{d_0} B_l \right]^{-1},$$

followed by the mean

$$\mu_l \leftarrow \frac{c_0}{d_0} A_l \sum_{\Omega} y_{i_1 \dots i_d} \left(\bigodot_{s \neq l} M_s^T g_{s,i_s} \right) \otimes g_{l,i_l}, \quad (10)$$

where M_s stands for the matricization of μ_s . We then update the rate parameters for the precision matrix

$$d_j \leftarrow b_j + \frac{1}{2} \sum_{l=1}^d \text{Tr} \{ \text{block}_j(\mu_l \mu_l^T + A_l) \} \quad (11)$$

for $j = 1, \dots, k$, and for the noise precision

$$\begin{aligned} d_0 \leftarrow b_0 + \frac{1}{2} \sum_{\Omega} & \left[y_{i_1 \dots i_d}^2 - 2y_{i_1 \dots i_d} \langle M_1^T g_{1,i_1}, \dots, M_d^T g_{d,i_d} \rangle \right. \\ & + \left\langle (I_k \otimes g_{1,i_1}^T) A_1 (I_k \otimes g_{1,i_1}) + M_s^T g_{s,i_s} g_{s,i_s}^T M_s, \dots, \right. \\ & \left. (I_k \otimes g_{d,i_d}^T) A_d (I_k \otimes g_{d,i_d}) + M_d^T g_{d,i_d} g_{d,i_d}^T M_d \right\rangle \Big]. \end{aligned} \quad (12)$$

The corresponding shape parameters have fixed values as shown above.

The missing entries of \mathbf{Y} follow, approximately, a Student's t -distribution

$$p(y_{i_1 \dots i_d} | \mathbf{Y}_{\Omega}) \approx \text{St}(y_{i_1 \dots i_d} | \langle M_1^T g_{1,i_1}, \dots, M_d^T g_{d,i_d} \rangle, \xi, 2c_0),$$

where ξ^{-1} equals

$$\frac{d_0}{c_0} + \sum_{l=1}^d \left(\bigodot_{s \neq l} M_s^T g_{s,i_s} \right)^T (I_k \otimes g_{l,i_l}^T) A_l (I_k \otimes g_{l,i_l}) \left(\bigodot_{s \neq l} M_s^T g_{s,i_s} \right),$$

giving mean $\langle M_1^T g_{1,i_1}, \dots, M_d^T g_{d,i_d} \rangle$ and variance $\frac{c_0}{\xi(c_0 - 1)}$.

5 Numerical experiments

5.1 Computational complexity

One step of our variational message passing algorithm consists in updating the parameters and hyperparameters of the posterior distributions, i.e. computing Eqs. (1)–(8) for matrix completion and Eqs. (9)–(12) for tensor completion.

Let $m = \max\{m_l\}$. Forming the matrix that needs to be inverted in (1) requires $\mathcal{O}(|\Omega|m^2k^2)$ operations. We then compute its Cholesky factorization, which takes $\mathcal{O}(m^3k^3)$ operations, and invert in $\mathcal{O}(m^2k^2)$. In (2), we can reuse the temporary vectors from (1) to compute the sum with $\mathcal{O}(|\Omega|mk)$ operations and multiply it by $A_{\bar{u}}$ using $\mathcal{O}(m^2k^2)$ operations, thanks to the Cholesky factorization. This results in $\mathcal{O}(|\Omega|m^2k^2 + m^3k^3)$ operations for updating the posterior distribution of one factor matrix. The cost of (6) is clearly dominated by that of factor matrix updates, and to compute the new d_0 via (8) requires $\mathcal{O}(|\Omega|m^2k^2)$ operations. So, in total, one iteration of variational message passing for matrix completion with side information takes $\mathcal{O}(|\Omega|m^2k^2 + m^3k^3)$ operations (cf. [13]).

In the tensor case, the asymptotic computational complexity is also defined by the updates for canonical factors. Each of them now costs $\mathcal{O}(d|\Omega|m^2k^2 + m^3k^3)$ operations, and added up together they give the total complexity of $\mathcal{O}(d^2|\Omega|m^2k^2 + dm^3k^3)$ operations.

This complexity can potentially be reduced, if we use a different strategy for matrix inversion, such as conjugate gradient or Newton iterations, or sparse Cholesky factorizations [80].

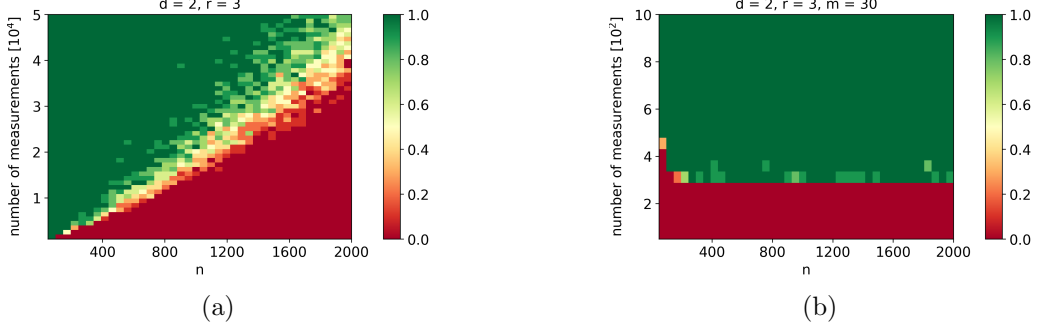


Figure 1: Phase plots for noiseless matrix completion with rank $r = 3$ and perfect rank prediction $k = 3$: FBCP (a) and FBCP-SI with side information size $m = 30$ (b).

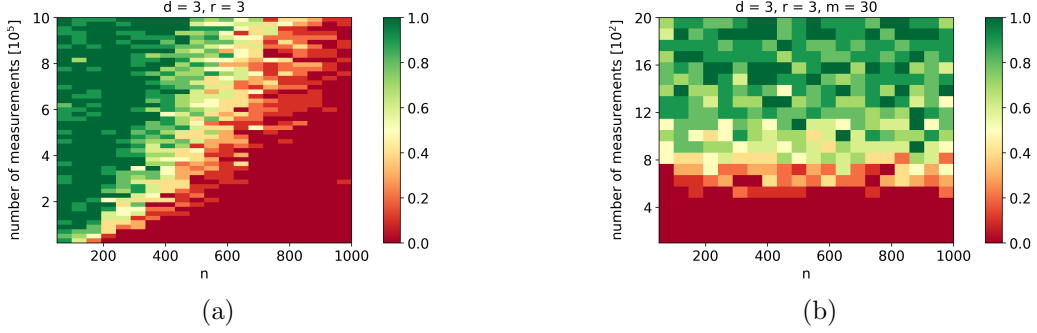


Figure 2: Phase plots for noiseless 3-dimensional CP completion with rank $r = 3$ and perfect rank prediction $k = 3$: FBCP (a) and FBCP-SI with side information size $m = 30$ (b).

5.2 Initialization

In all our experiments we initialize the posterior rate and shape $(\{c_j, d_j\})$ and (c_0, d_0) of the precision parameters with 10^{-6} . We draw the posterior means $\{\mu_l\}$ of the factor matrices from the standard Gaussian distribution $\mathcal{N}(0, I)$ and set their covariances $\{A_l\}$ to identities I ; it is also possible to initialize using SVD [62].

5.3 Synthetic data

To extensively test the regularization properties of side information, we generate random data. For fixed values of d , n , m , and r , we draw d latent factors $\{U_l\}$ of sizes $m \times r$ with i.i.d elements from $\mathcal{N}(0, 1)$. The side information matrices $\{G_l\}$ of sizes $n \times m$ are generated in the same way. If no side information is used, we generate $\{U_l\}$ of sizes $n \times r$. We denote an instance of such tensors by $\mathbf{X}(d, n, r, m)$ and $\mathbf{X}(d, n, r)$, respectively. The sampling set Ω is chosen uniformly at random with replacement from $[n]^d$. The noise is Gaussian with zero mean and variance that gives the prescribed signal-to-noise ratio (SNR).

5.3.1 Performance of completion

In the first series of experiments, which are presented in Figs. 1 and 2, we study how side information can reduce the number of elements $|\Omega|$ needed to recover a low-rank CP tensor with FBCP [62]. For every set of parameters, we generate N_{trial} random problems

$$\left\{ \mathbf{X}^{(t)}(d, n, r), \Omega^{(t)}, \Omega_{test}^{(t)} \right\}_{t=1}^{N_{trial}}$$

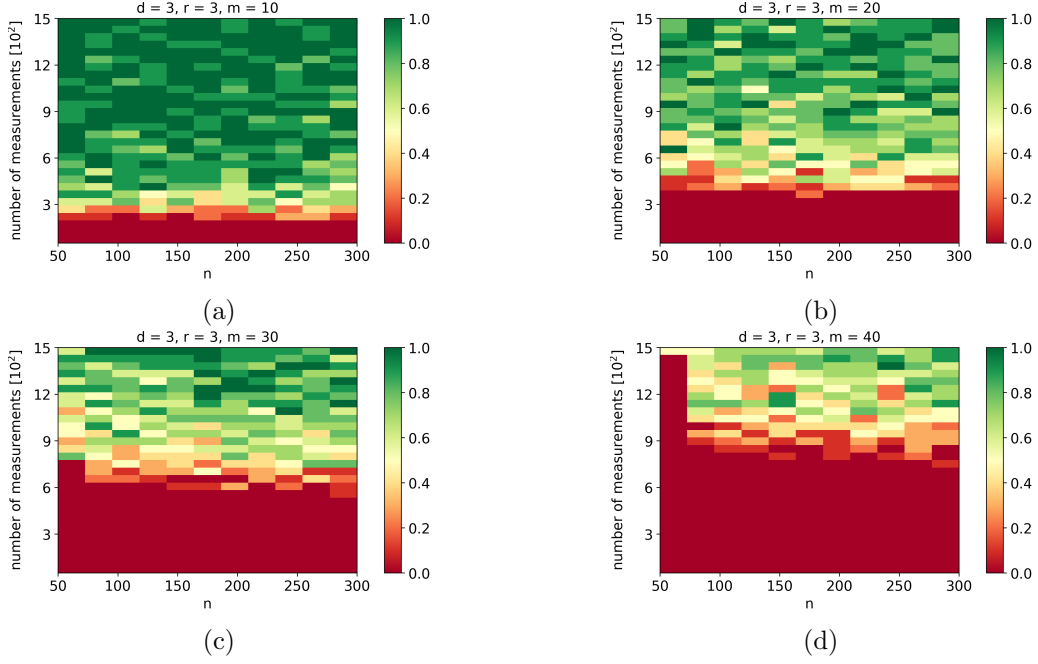


Figure 3: Phase plots for noiseless 3-dimensional CP completion with rank $r = 3$, perfect rank prediction $k = 3$, and different sizes of side information: $m = 10$ (a), $m = 20$ (b), $m = 30$ (c), and $m = 40$ (d).

without noise and run N_{iter} iterations of FBCP with N_{ic} different random initial conditions with perfect rank prediction $k = r$. We say that a problem is successfully solved if RMSE on a test sampling set $\Omega_{test}^{(t)}$ of size $|\Omega|$ is smaller than 10^{-6} :

$$\frac{\left\| \mathcal{P}_{\Omega_{test}^{(t)}} \left(\mathbf{X}^{(t)} - \mathbf{X}_{N_{iter}}^{(t)} \right) \right\|_F}{\left\| \mathcal{P}_{\Omega_{test}^{(t)}} \mathbf{X}^{(t)} \right\|_F} < 10^{-6}.$$

We then plot the frequency of successes among the $N_{trial}N_{ic}$ runs in the $(n, |\Omega|)$ -plane. In the same way, we test our method, FBCP with side information (FBCP-SI), by generating

$$\left\{ \mathbf{X}^{(t)}(d, n, r, m), \Omega^{(t)}, \Omega_{test}^{(t)} \right\}_{t=1}^{N_{trial}}.$$

We show the phase plots for $d = 2$, $r = 3$, $m = 30$ (Fig. 1) and $d = 3$, $r = 3$, $m = 30$ (Fig. 2). In both cases we made $N_{trial} = 5$ trials with $N_{ic} = 2$ different initial conditions, making $N_{iter} = 100$ iterations for $d = 2$ and $N_{iter} = 150$ iterations for $d = 3$. In the presence of side information, the phase transition curve for CP completion becomes horizontal, i.e. the critical size of $|\Omega|$ that makes completion possible is essentially independent of n and, hence, greatly reduced. Indeed, a rank-3 CP tensor of size $300 \times 300 \times 300$ can be completed from 1% of its elements, and only 0.004% are needed when 30-dimensional side-information subspaces are available for all of its fibers (columns, rows, and tubes); for a larger $1000 \times 1000 \times 1000$ tensor with the same side information this reduces to 0.0001%. Similar behavior has been observed for Riemannian TT completion with side information [75].

Looking closely at Figs. 1 and 2, we can note that the phase transition curves have a bump for small values of n (in fact, it is seen in the phase plots for TT completion as well [75] but remained unnoticed). We explore this phenomenon by zooming in on the phase plots for $d = 3$,

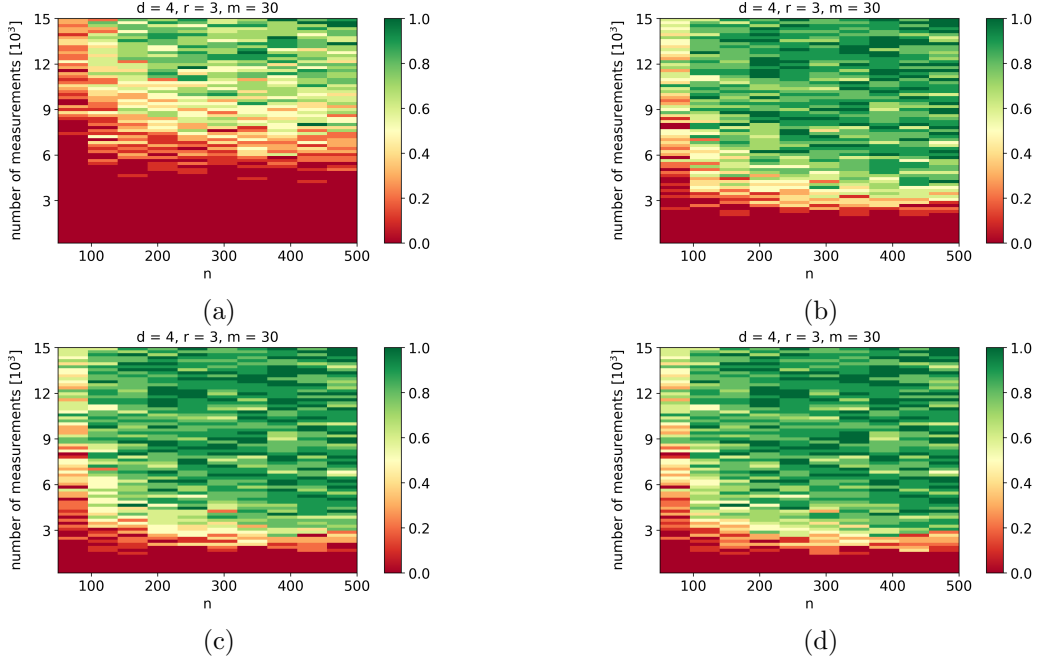


Figure 4: Phase plots for noiseless 4-dimensional CP completion with rank $r = 3$, perfect rank prediction $k = 3$, and side information size $m = 30$ after different numbers of iterations: $N_{iter} = 20$ (a), $N_{iter} = 50$ (b), $N_{iter} = 100$ (c), and $N_{iter} = 200$ (d).

$r = 3$, and different values of m (Fig. 3). The numerical results suggest that the bump occurs for m comparable with n and is absent when it is sufficiently small.

A possible explanation of the bump's existence is that FBCP-SI might require more iterations to converge when $m \lesssim n$. To check this, we carry out experiments for $d = 4$, $r = 3$, $m = 30$ with perfect rank prediction $k = 3$, $N_{trial} = 5$, $N_{ic} = 2$, and present the corresponding phase plots for different values of N_{iter} , ranging from 20 to 200 iterations; see Fig. 4. We see that even for $n = 100$ the threshold value of $|\Omega|$ descends rapidly with iterations and stabilizes after $N_{iter} = 50$. Meanwhile, the bump exists for $n = 50$ and persists nearly unchanged throughout 200 iterations. These results suggest that early stopping is likely not what keeps the phase transition curve from being completely horizontal. See Discussion for more thoughts about the bump.

5.3.2 Performance of rank determination

In the previous examples, we assumed that the CP-rank was given in advance, i.e. the predicted rank k was always equal to the true rank r . In the following experiments, we consider a more realistic scenario where only an upper bound of the rank is known. To test automatic rank determination of FBCP-SI, we generated random rank-3 CP tensors of size $100 \times 100 \times 100$ and ran $N_{iter} = 100$ iterations with $k = 10$ for different values of $|\Omega|$ and various levels of noise. We determine the rank based on the posterior means of the hyperparameters $\{\lambda_j\}$ and a threshold parameter $\varepsilon > 0$:

$$r_\varepsilon = \left| \left\{ j : j \in [k], \frac{d_j}{c_j} \geq \varepsilon \max_{i \in [k]} \frac{d_i}{c_i} \right\} \right|.$$

We plot the rank r_ε , averaged over $N_{trial} = 20$ trials with $N_{ic} = 1$, against SNR for different values of ε ; see Figs. 5 and 6 with $m = 10$ and $m = 30$, respectively. Comparing the two Figs., we see that given the same number of samples $|\Omega|$, lower dimension of side information

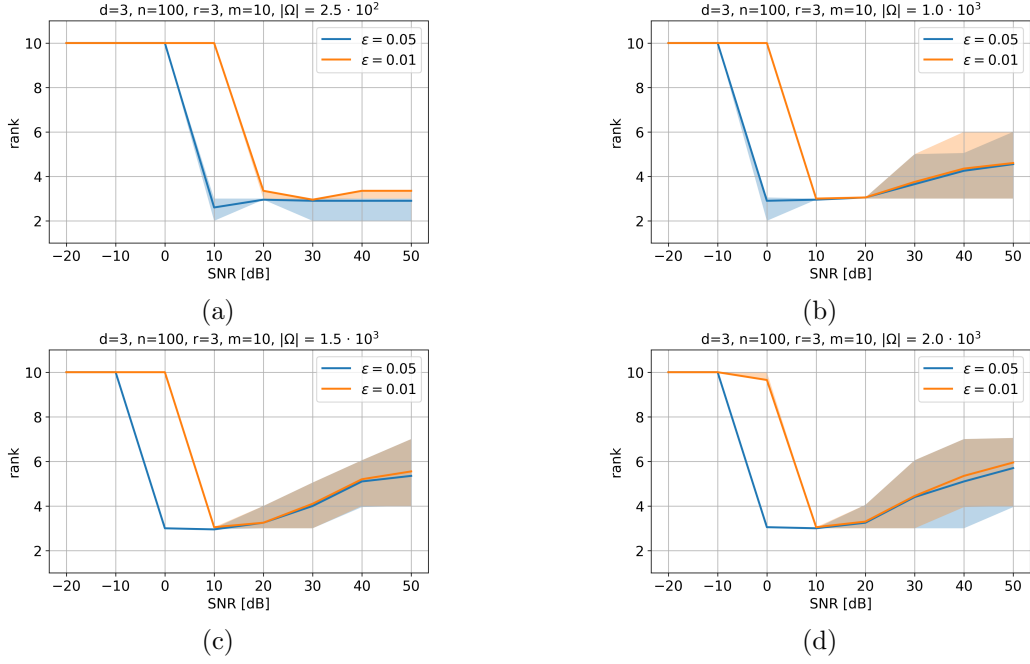


Figure 5: Determined rank for 3-dimensional CP completion with size $n = 100$, rank $r = 3$, side information size $m = 10$, rank prediction $k = 10$, varying levels of noise and different numbers of samples: $|\Omega| = 2.5 \cdot 10^2$ (a), $|\Omega| = 1 \cdot 10^3$ (b), $|\Omega| = 1.5 \cdot 10^3$ (c), and $|\Omega| = 2 \cdot 10^3$ (d). The curves show the averaged rank together with the 5th and 95th percentiles for threshold values $\varepsilon = 0.05$ and $\varepsilon = 0.01$.

subspaces leads to better rank determination at SNR of 0dB; however, at the same time, the rank tends to be overestimated for high SNR.

Find more experiments with synthetic data in the Appendix.

5.4 Facial images

To verify the performance of our algorithm on real-world data, we used the 3D Basel Face Model [81]: a collection of facial images of 10 people, taken from 9 angles under 3 light settings. We cropped and rescaled each image to 70×70 pixels.

For the first experiment, we pick out one person and consider her portraits as a $4900 \times 3 \times 9$ tensor. We choose $m_1 = 9$, $m_2 = 3$, and $m_3 = 9$, with the side information subspace for ‘faces’ spanned by the 9 first singular vectors of the 4900×27 flattening. In Table 1, we compare how FBCP and FBCP-SI find a rank-10 approximation of the data when all 27 portraits are known and when 7 of them, chosen at random, are missing. In the approximation case (all portraits are known), FBCP-SI shows better accuracy both in RMSE and SSIM metrics. In the completion case, FBCP-SI recovers the missing images worse than FBCP: it struggles in complete accordance with the bump phenomenon that we saw in synthetic experiments, since $m_2 = n_2$.

We check this in the second experiment, where we keep only 9 images out of 27: one per angle. We compare three methods: FBCP, FBCP-SI with the same parameters as above, and FBCP-SI with m_2 reduced to 1. For the latter, the side information subspace is learnt from the 9 other people in the dataset as the dominant left singular vector of their $3 \times (4900 \cdot 9 \cdot 9)$ flattening. The results are presented in Table 2. We see that FBCP-SI with $m_2 = 1$ succeeds in recovering 18 missing images, while FBCP and FBCP-SI with $m_2 = 3$ fail to do so (see Fig. 7).

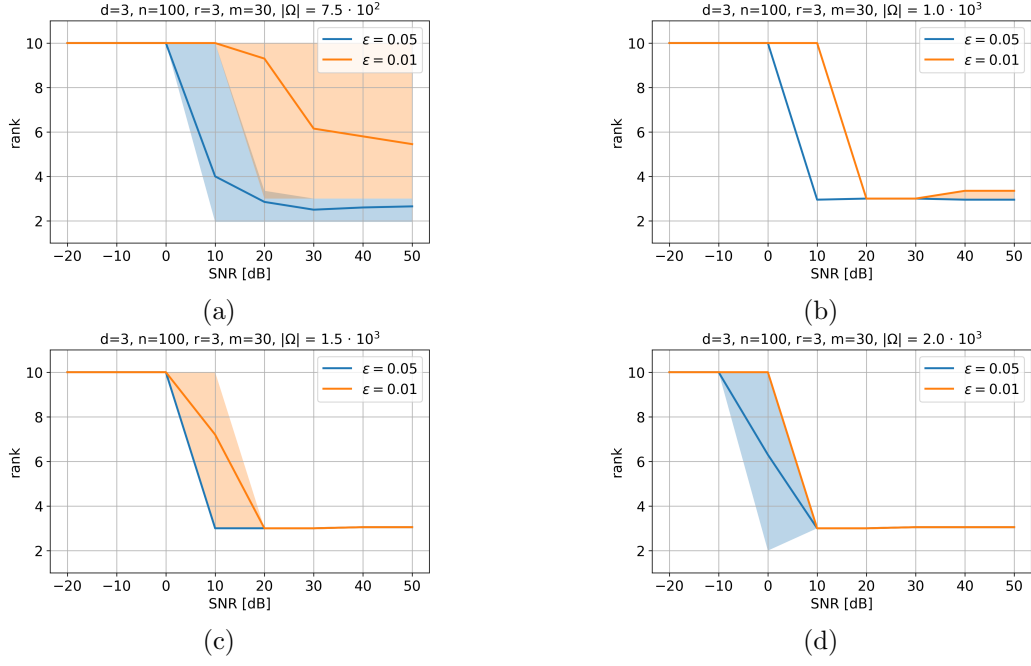


Figure 6: Determined rank for 3-dimensional CP completion with size $n = 100$, rank $r = 3$, side information size $m = 30$, rank prediction $k = 10$, varying levels of noise and different numbers of samples: $|\Omega| = 2.5 \cdot 10^2$ (a), $|\Omega| = 1 \cdot 10^3$ (b), $|\Omega| = 1.5 \cdot 10^3$ (c), and $|\Omega| = 2 \cdot 10^3$ (d). The curves show the averaged rank together with the 5th and 95th percentiles for threshold values $\varepsilon = 0.05$ and $\varepsilon = 0.01$.

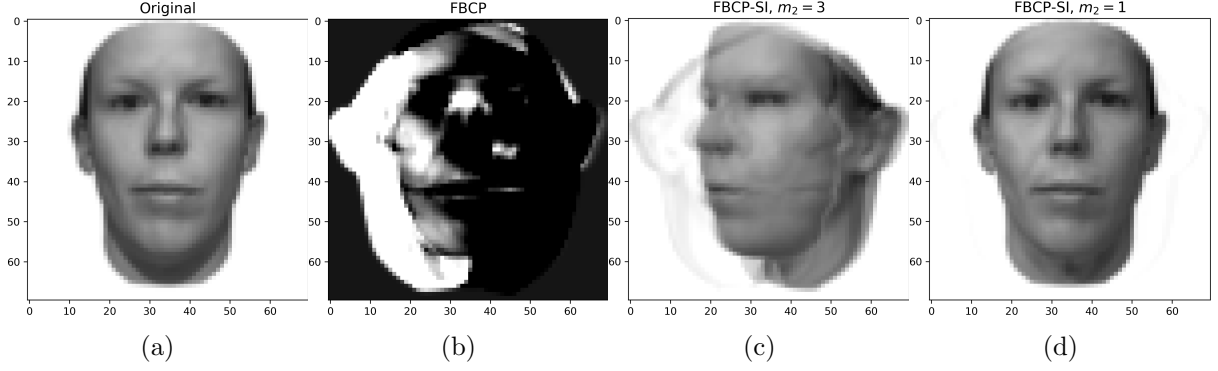


Figure 7: An example of a recovered image from the 3D Basel Face Model by rank-10 $4900 \times 3 \times 9$ tensor completion, when 1 out of 3 images are known for each angle: original (a); FBCP (b); FBCP-SI with $m_1 = 9$, $m_2 = 3$, $m_3 = 9$ (c); FBCP-SI with $m_1 = 9$, $m_2 = 1$, $m_3 = 9$ (d).

Table 1: The results of rank-10 $4900 \times 3 \times 9$ CP completion for the 3D Basel Face Model by FBCP and FBCP-SI with $m_1 = 9$, $m_2 = 3$, $m_3 = 9$.

Observed	Method	RMSE		SSIM	
		Obs.	Miss.	Obs.	Miss.
27/27	FBCP	0.04	N/A	0.91	N/A
	FBCP-SI	0.03	N/A	0.97	N/A
20/27	FBCP	0.05	0.09	0.90	0.81
	FBCP-SI	0.04	0.22	0.91	0.61

Table 2: The results of rank-10 $4900 \times 3 \times 9$ CP completion for the 3D Basel Face Model, when 1 out of 3 images are known for each angle: FBCP; FBCP-SI with $m_1 = 9$, $m_2 = 3$, $m_3 = 9$; FBCP-SI with $m_1 = 9$, $m_2 = 1$, $m_3 = 9$.

Method	RMSE		SSIM	
	Obs.	Miss.	Obs.	Miss.
FBCP	0.08	0.96	0.86	0.26
FBCP-SI, $m_2 = 3$	1.00	0.82	0.001	0.09
FBCP-SI, $m_2 = 1$	0.04	0.07	0.91	0.88

6 Discussion

We considered the problem of low-rank CP tensor completion with side information in the Bayesian framework. Having fixed a probabilistic model, we derived formulas for variational approximate Bayesian inference and the corresponding message passing algorithm. The results of numerical experiments allow us to analyze the regularization properties induced by side information: how it affects the phase plots, the rate of convergence, the attainable errors in the presence of noise, and automatic rank determination. The strongest point of our algorithm is that it significantly reduces the number of elements needed for successful completion of a tensor. For instance, a rank-3 CP tensor of size $300 \times 300 \times 300$ can be recovered from 1% of its entries without side information and from only 0.004% if there is 30-dimensional side information. This suggests that our method can be useful for applications where data are exceptionally scarce.

We would also like to add a few words about the bump in the phase transition curves that we observed for $m \lesssim n$. In [75], such bump can be recognized on the phase plot corresponding to Riemannian tensor train completion with side information of a 10-dimensional tensor. At the same time, the results of [76] tell us that Riemannian gradient descent converges *locally* if the number of samples $|\Omega|$ exceeds a certain threshold that depends on m and is independent of n , and this behavior is indeed seen on the phase plots for larger values of n . However, random initialization that is used in [75] (and in this paper too) certainly does not put the initial condition into the basin of local attraction. Recent results on non-convex optimization [82–84] show that gradient descent converges *globally* in certain problems (including matrix completion) when initialized randomly, provided, of course, that $|\Omega|$ is large enough. So the existence of the bump could find its explanation in the delicate analysis of global convergence from a random initial point for tensor completion with side information: it is possible that the threshold value of $|\Omega|$ that guarantees global convergence depends on n when $m \lesssim n$.

Acknowledgements

This work was supported by Russian Science Foundation (project 21-71-10072).

References

- [1] D. L. Donoho. Compressed sensing. *IEEE Transactions on Information Theory*, 52(4):1289–1306, April 2006.
- [2] Emmanuel J. Candès and Benjamin Recht. Exact Matrix Completion via Convex Optimization. *Foundations of Computational Mathematics*, 9(6):717, April 2009.
- [3] Emmanuel J. Candès and Terence Tao. The Power of Convex Relaxation: Near-Optimal Matrix Completion. *IEEE Transactions on Information Theory*, 56(5):2053–2080, May 2010.
- [4] Emmanuel J. Candès, Xiaodong Li, Yi Ma, and John Wright. Robust principal component analysis? *Journal of the ACM*, 58(3):1–37, May 2011.
- [5] João F. C. Mota, Nikos Deligiannis, and Miguel R. D. Rodrigues. Compressed Sensing With Prior Information: Strategies, Geometry, and Bounds. *IEEE Transactions on Information Theory*, 63(7):4472–4496, July 2017.

- [6] Niannan Xue, Yannis Panagakis, and Stefanos Zafeiriou. Side Information in Robust Principal Component Analysis: Algorithms and Applications. In *Proceedings of the IEEE International Conference on Computer Vision*, pages 4317–4325, 2017.
- [7] Nikhil Rao, Hsiang-Fu Yu, Pradeep K Ravikumar, and Inderjit S Dhillon. Collaborative Filtering with Graph Information: Consistency and Scalable Methods. In *Advances in Neural Information Processing Systems*, volume 28. Curran Associates, Inc., 2015.
- [8] Nauman Shahid, Nathanael Perraudin, Vassilis Kalofolias, Gilles Puy, and Pierre Vandergheynst. Fast Robust PCA on Graphs. *IEEE Journal of Selected Topics in Signal Processing*, 10(4):740–756, June 2016.
- [9] Ajit P. Singh and Geoffrey J. Gordon. Relational learning via collective matrix factorization. In *Proceedings of the 14th ACM SIGKDD International Conference on Knowledge Discovery and Data Mining*, KDD ’08, pages 650–658, New York, NY, USA, August 2008. Association for Computing Machinery.
- [10] Hanhuai Shan and Arindam Banerjee. Generalized Probabilistic Matrix Factorizations for Collaborative Filtering. In *2010 IEEE International Conference on Data Mining*, pages 1025–1030, December 2010.
- [11] Prateek Jain and Inderjit S. Dhillon. Provable Inductive Matrix Completion. *arXiv:1306.0626 [cs, math, stat]*, June 2013.
- [12] Miao Xu, Rong Jin, and Zhi-Hua Zhou. Speedup Matrix Completion with Side Information: Application to Multi-Label Learning. In C. J. C. Burges, L. Bottou, M. Welling, Z. Ghahramani, and K. Q. Weinberger, editors, *Advances in Neural Information Processing Systems 26*, pages 2301–2309. Curran Associates, Inc., 2013.
- [13] Yong-Deok Kim and Seungjin Choi. Scalable Variational Bayesian Matrix Factorization with Side Information. In *Proceedings of the Seventeenth International Conference on Artificial Intelligence and Statistics*, pages 493–502. PMLR, April 2014.
- [14] Kai-Yang Chiang, Cho-Jui Hsieh, and Inderjit S Dhillon. Matrix Completion with Noisy Side Information. In C. Cortes, N. D. Lawrence, D. D. Lee, M. Sugiyama, and R. Garnett, editors, *Advances in Neural Information Processing Systems 28*, pages 3447–3455. Curran Associates, Inc., 2015.
- [15] Kai-Yang Chiang, Cho-Jui Hsieh, and Inderjit Dhillon. Robust Principal Component Analysis with Side Information. In *Proceedings of The 33rd International Conference on Machine Learning*, pages 2291–2299. PMLR, June 2016.
- [16] Hao Ma, Haixuan Yang, Michael R. Lyu, and Irwin King. SoRec: Social recommendation using probabilistic matrix factorization. In *Proceedings of the 17th ACM Conference on Information and Knowledge Management*, CIKM ’08, pages 931–940, New York, NY, USA, October 2008. Association for Computing Machinery.
- [17] Hong-Bo Xie, Caoyuan Li, Richard Yi Da Xu, and Kerrie Mengersen. Robust Kernelized Bayesian Matrix Factorization for Video Background/Foreground Separation. In Giuseppe Nicosia, Panos Pardalos, Renato Umeton, Giovanni Giuffrida, and Vincenzo Sciacca, editors, *Machine Learning, Optimization, and Data Science*, Lecture Notes in Computer Science, pages 484–495, Cham, 2019. Springer International Publishing.

- [18] Nagarajan Natarajan and Inderjit S. Dhillon. Inductive matrix completion for predicting gene–disease associations. *Bioinformatics*, 30(12):i60–i68, June 2014.
- [19] Pooya Zakeri, Jaak Simm, Adam Arany, Sarah ElShal, and Yves Moreau. Gene prioritization using Bayesian matrix factorization with genomic and phenotypic side information. *Bioinformatics*, 34(13):i447–i456, July 2018.
- [20] Betül Güvenç Paltun, Hiroshi Mamitsuka, and Samuel Kaski. Improving drug response prediction by integrating multiple data sources: Matrix factorization, kernel and network-based approaches. *Briefings in Bioinformatics*, 22(1):346–359, January 2021.
- [21] Tamara G. Kolda and Brett W. Bader. Tensor Decompositions and Applications. *SIAM Review*, 51(3):455–500, August 2009.
- [22] I. V. Oseledets. Tensor-Train Decomposition. *SIAM Journal on Scientific Computing*, 33(5):2295–2317, January 2011.
- [23] Andrzej Cichocki, Danilo Mandic, Lieven De Lathauwer, Guoxu Zhou, Qibin Zhao, Cesar Caiafa, and Huy Anh Phan. Tensor Decompositions for Signal Processing Applications: From two-way to multiway component analysis. *IEEE Signal Processing Magazine*, 32(2):145–163, March 2015.
- [24] Evangelos E. Papalexakis, Christos Faloutsos, and Nicholas D. Sidiropoulos. Tensors for Data Mining and Data Fusion: Models, Applications, and Scalable Algorithms. *ACM Transactions on Intelligent Systems and Technology*, 8(2):16:1–16:44, October 2016.
- [25] Nicholas D. Sidiropoulos, Lieven De Lathauwer, Xiao Fu, Kejun Huang, Evangelos E. Papalexakis, and Christos Faloutsos. Tensor Decomposition for Signal Processing and Machine Learning. *IEEE Transactions on Signal Processing*, 65(13):3551–3582, July 2017.
- [26] Marco Signoretto, Lieven De Lathauwer, and Johan A. K. Suykens. Nuclear Norms for Tensors and Their Use for Convex Multilinear Estimation. *Submitted to Linear Algebra and Its Applications*, 43, 2010.
- [27] Silvia Gandy, Benjamin Recht, and Isao Yamada. Tensor completion and low-n-rank tensor recovery via convex optimization. *Inverse Problems*, 27(2):025010, January 2011.
- [28] Johann A. Bengua, Ho N. Phien, Hoang Duong Tuan, and Minh N. Do. Efficient Tensor Completion for Color Image and Video Recovery: Low-Rank Tensor Train. *IEEE Transactions on Image Processing*, 26(5):2466–2479, May 2017.
- [29] Jared. Tanner and Ke. Wei. Normalized Iterative Hard Thresholding for Matrix Completion. *SIAM Journal on Scientific Computing*, 35(5):S104–S125, January 2013.
- [30] O. S. Lebedeva, A. I. Osinsky, and S. V. Petrov. Low-Rank Approximation Algorithms for Matrix Completion with Random Sampling. *Computational Mathematics and Mathematical Physics*, 61(5):799–815, May 2021.
- [31] Holger Rauhut, Reinhold Schneider, and Željka Stojanac. Tensor Completion in Hierarchical Tensor Representations. In Holger Boche, Robert Calderbank, Gitta Kutyniok, and Jan Vybíral, editors, *Compressed Sensing and Its Applications: MATHEON Workshop 2013*, Applied and Numerical Harmonic Analysis, pages 419–450. Springer International Publishing, Cham, 2015.

- [32] Justin P. Haldar and Diego Hernando. Rank-Constrained Solutions to Linear Matrix Equations Using PowerFactorization. *IEEE Signal Processing Letters*, 16(7):584–587, July 2009.
- [33] Zaiwen Wen, Wotao Yin, and Yin Zhang. Solving a low-rank factorization model for matrix completion by a nonlinear successive over-relaxation algorithm. *Mathematical Programming Computation*, 4(4):333–361, December 2012.
- [34] Prateek Jain, Praneeth Netrapalli, and Sujay Sanghavi. Low-rank matrix completion using alternating minimization. In *Proceedings of the Forty-Fifth Annual ACM Symposium on Theory of Computing*, STOC ’13, pages 665–674, New York, NY, USA, June 2013. Association for Computing Machinery.
- [35] Trevor Hastie, Rahul Mazumder, Jason D. Lee, and Reza Zadeh. Matrix Completion and Low-Rank SVD via Fast Alternating Least Squares. *Journal of machine learning research: JMLR*, 16:3367–3402, 2015.
- [36] Jared Tanner and Ke Wei. Low rank matrix completion by alternating steepest descent methods. *Applied and Computational Harmonic Analysis*, 40(2):417–429, March 2016.
- [37] Lars. Grasedyck, Melanie. Kluge, and Sebastian. Krämer. Variants of Alternating Least Squares Tensor Completion in the Tensor Train Format. *SIAM Journal on Scientific Computing*, 37(5):A2424–A2450, January 2015.
- [38] Lars Grasedyck and Sebastian Krämer. Stable ALS approximation in the TT-format for rank-adaptive tensor completion. *Numerische Mathematik*, 143(4):855–904, December 2019.
- [39] Raghunandan H. Keshavan, Andrea Montanari, and Sewoong Oh. Matrix Completion From a Few Entries. *IEEE Transactions on Information Theory*, 56(6):2980–2998, June 2010.
- [40] Nicolas Boumal and P. A. Absil. RTRMC: A Riemannian trust-region method for low-rank matrix completion. In *Advances in Neural Information Processing Systems 24: 25th Annual Conference on Neural Information Processing Systems 2011, NIPS 2011*, December 2011.
- [41] Bart. Vandereycken. Low-Rank Matrix Completion by Riemannian Optimization. *SIAM Journal on Optimization*, 23(2):1214–1236, January 2013.
- [42] Bamdev Mishra, Gilles Meyer, Silvere Bonnabel, and Rodolphe Sepulchre. Fixed-rank matrix factorizations and Riemannian low-rank optimization. *Computational Statistics*, 29(3):591–621, June 2014.
- [43] Daniel Kressner, Michael Steinlechner, and Bart Vandereycken. Low-rank tensor completion by Riemannian optimization. *BIT Numerical Mathematics*, 54(2):447–468, June 2014.
- [44] Michael. Steinlechner. Riemannian Optimization for High-Dimensional Tensor Completion. *SIAM Journal on Scientific Computing*, 38(5):S461–S484, January 2016.
- [45] Vin de Silva and Lek-Heng Lim. Tensor Rank and the Ill-Posedness of the Best Low-Rank Approximation Problem. *SIAM Journal on Matrix Analysis and Applications*, 30(3):1084–1127, January 2008.
- [46] Giorgio Tomasi and Rasmus Bro. PARAFAC and missing values. *Chemometrics and Intelligent Laboratory Systems*, 75(2):163–180, February 2005.

- [47] Evrim Acar, Daniel M. Dunlavy, Tamara G. Kolda, and Morten Mørup. Scalable tensor factorizations for incomplete data. *Chemometrics and Intelligent Laboratory Systems*, 106(1):41–56, March 2011.
- [48] Tatsuya Yokota, Qibin Zhao, and Andrzej Cichocki. Smooth PARAFAC Decomposition for Tensor Completion. *IEEE Transactions on Signal Processing*, 64(20):5423–5436, October 2016.
- [49] Ruslan Salakhutdinov and Andriy Mnih. Probabilistic Matrix Factorization. In *Advances in Neural Information Processing Systems*, volume 20. Curran Associates, Inc., 2007.
- [50] Radford M. Neal. Probabilistic Inference Using Markov Chain Monte Carlo Methods. Technical Report CRG-TR-93-1, University of Toronto, Department of Computer Science, 1993.
- [51] Matthew James Beal. *Variational Algorithms for Approximate Bayesian Inference*. PhD thesis, University College London, 2003.
- [52] John Winn and Christopher M. Bishop. Variational Message Passing. *The Journal of Machine Learning Research*, 6:661–694, December 2005.
- [53] Ruslan Salakhutdinov and Andriy Mnih. Bayesian probabilistic matrix factorization using Markov chain Monte Carlo. In *Proceedings of the 25th International Conference on Machine Learning, ICML '08*, pages 880–887, New York, NY, USA, July 2008. Association for Computing Machinery.
- [54] Daniel E. Gilbert and Martin T. Wells. Tuning Free Rank-Sparse Bayesian Matrix and Tensor Completion with Global-Local Priors. *arXiv:1905.11496 [stat]*, May 2019.
- [55] Balaji Lakshminarayanan, Guillaume Bouchard, and Cedric Archambeau. Robust Bayesian Matrix Factorisation. In *Proceedings of the Fourteenth International Conference on Artificial Intelligence and Statistics*, pages 425–433. JMLR Workshop and Conference Proceedings, June 2011.
- [56] S. Derin Babacan, Martin Luessi, Rafael Molina, and Aggelos K. Katsaggelos. Sparse Bayesian Methods for Low-Rank Matrix Estimation. *IEEE Transactions on Signal Processing*, 60(8):3964–3977, August 2012.
- [57] Linxiao Yang, Jun Fang, Huiping Duan, Hongbin Li, and Bing Zeng. Fast Low-Rank Bayesian Matrix Completion With Hierarchical Gaussian Prior Models. *IEEE Transactions on Signal Processing*, 66(11):2804–2817, June 2018.
- [58] Wei Chu and Zoubin Ghahramani. Probabilistic Models for Incomplete Multi-dimensional Arrays. In *Proceedings of the Twelfth International Conference on Artificial Intelligence and Statistics*, pages 89–96. PMLR, April 2009.
- [59] Qibin Zhao, Liqing Zhang, and Andrzej Cichocki. Bayesian Sparse Tucker Models for Dimension Reduction and Tensor Completion. *arXiv:1505.02343 [cs, stat]*, May 2015.
- [60] Le Xu, Lei Cheng, Ngai Wong, and Yik-Chung Wu. Learning Tensor Train Representation with Automatic Rank Determination from Incomplete Noisy Data. *arXiv:2010.06564 [eess]*, October 2020.

- [61] Piyush Rai, Yingjian Wang, Shengbo Guo, Gary Chen, David Dunson, and Lawrence Carin. Scalable Bayesian Low-Rank Decomposition of Incomplete Multiway Tensors. In *Proceedings of the 31st International Conference on Machine Learning*, pages 1800–1808. PMLR, June 2014.
- [62] Qibin Zhao, Liqing Zhang, and Andrzej Cichocki. Bayesian CP Factorization of Incomplete Tensors with Automatic Rank Determination. *IEEE Transactions on Pattern Analysis and Machine Intelligence*, 37(9):1751–1763, September 2015.
- [63] Qibin Zhao, Guoxu Zhou, Liqing Zhang, Andrzej Cichocki, and Shun-Ichi Amari. Bayesian Robust Tensor Factorization for Incomplete Multiway Data. *IEEE Transactions on Neural Networks and Learning Systems*, 27(4):736–748, April 2016.
- [64] Lei Cheng, Zhongtao Chen, Qingjiang Shi, Yik-Chung Wu, and Sergios Theodoridis. Towards Probabilistic Tensor Canonical Polyadic Decomposition 2.0: Automatic Tensor Rank Learning Using Generalized Hyperbolic Prior. *arXiv:2009.02472 [cs, eess, stat]*, September 2020.
- [65] Pierre Alquier, Vincent Cottet, Nicolas Chopin, and Judith Rousseau. Bayesian matrix completion: Prior specification. *arXiv:1406.1440 [math, stat]*, October 2014.
- [66] Evrim Acar, Tamara G. Kolda, and Daniel M. Dunlavy. All-at-once Optimization for Coupled Matrix and Tensor Factorizations. *arXiv:1105.3422 [physics, stat]*, May 2011.
- [67] Atsuhiko Narita, Kohei Hayashi, Ryota Tomioka, and Hisashi Kashima. Tensor factorization using auxiliary information. *Data Mining and Knowledge Discovery*, 25(2):298–324, September 2012.
- [68] Tatsuya Yokota, Andrzej Cichocki, and Yukihiro Yamashita. Linked PARAFAC/CP Tensor Decomposition and Its Fast Implementation for Multi-block Tensor Analysis. In Tingwen Huang, Zhigang Zeng, Chuandong Li, and Chi Sing Leung, editors, *Neural Information Processing*, Lecture Notes in Computer Science, pages 84–91, Berlin, Heidelberg, 2012. Springer.
- [69] Juan Andrés Bazerque, Gonzalo Mateos, and Georgios B. Giannakis. Rank Regularization and Bayesian Inference for Tensor Completion and Extrapolation. *IEEE Transactions on Signal Processing*, 61(22):5689–5703, November 2013.
- [70] Yuankai Wu, Huachun Tan, Yong Li, Jian Zhang, and Xiaoxuan Chen. A Fused CP Factorization Method for Incomplete Tensors. *IEEE Transactions on Neural Networks and Learning Systems*, 30(3):751–764, March 2019.
- [71] Yu Guan, Shuyu Dong, P.-A. Absil, and François Glineur. Alternating minimization algorithms for graph regularized tensor completion. *arXiv:2008.12876 [cs, math]*, August 2020.
- [72] Vassilis N. Ioannidis, Ahmed S. Zamzam, Georgios B. Giannakis, and Nicholas D. Sidiropoulos. Coupled Graphs and Tensor Factorization for Recommender Systems and Community Detection. *IEEE Transactions on Knowledge and Data Engineering*, 33(3):909–920, March 2021.
- [73] Chaoqi Yang, Navjot Singh, Cao Xiao, Cheng Qian, Edgar Solomonik, and Jimeng Sun. MTC: Multiresolution Tensor Completion from Partial and Coarse Observations. *arXiv:2106.07135 [cs, math]*, June 2021.

- [74] Beyza Ermiş, Evrim Acar, and A. Taylan Cemgil. Link prediction in heterogeneous data via generalized coupled tensor factorization. *Data Mining and Knowledge Discovery*, 29(1):203–236, January 2015.
- [75] Stanislav Budzinskiy and Nikolai Zamarashkin. Note: Low-rank tensor train completion with side information based on Riemannian optimization. *arXiv:2006.12798 [cs, math]*, June 2020.
- [76] Stanislav Budzinskiy and Nikolai Zamarashkin. Tensor train completion: Local recovery guarantees via Riemannian optimization. *arXiv:2110.03975 [cs, math]*, October 2021.
- [77] Zhen Long, Ce Zhu, Jiani Liu, Pierre Comon, and Yipeng Liu. Trainable subspaces for low rank tensor completion: Model and analysis. *IEEE Transactions on Signal Processing*, 70:2502–2517, 2022.
- [78] Mehmet Gönen, Suleiman Khan, and Samuel Kaski. Kernelized Bayesian Matrix Factorization. In *Proceedings of the 30th International Conference on Machine Learning*, pages 864–872. PMLR, May 2013.
- [79] Caoyuan Li, Hong-Bo Xie, Xuhui Fan, Richard Yi Da Xu, Sabine Van Huffel, and Kerrie Mengersen. Kernelized Sparse Bayesian Matrix Factorization. *IEEE Transactions on Neural Networks and Learning Systems*, 32(1):391–404, January 2021.
- [80] Florian Schäfer, Matthias Katzfuss, and Houman Owhadi. Sparse Cholesky Factorization by Kullback–Leibler Minimization. *SIAM Journal on Scientific Computing*, 43(3):A2019–A2046, January 2021.
- [81] Pascal Paysan, Reinhard Knothe, Brian Amberg, Sami Romdhani, and Thomas Vetter. A 3d face model for pose and illumination invariant face recognition. In *2009 sixth IEEE international conference on advanced video and signal based surveillance*, pages 296–301. Ieee, 2009.
- [82] Yuxin Chen, Yuejie Chi, Jianqing Fan, and Cong Ma. Gradient descent with random initialization: Fast global convergence for nonconvex phase retrieval. *Mathematical Programming*, 176(1):5–37, July 2019.
- [83] Y. Chi, Y. M. Lu, and Y. Chen. Nonconvex Optimization Meets Low-Rank Matrix Factorization: An Overview. *IEEE Transactions on Signal Processing*, 67(20):5239–5269, October 2019.
- [84] Cong Ma, Kaizheng Wang, Yuejie Chi, and Yuxin Chen. Implicit Regularization in Nonconvex Statistical Estimation: Gradient Descent Converges Linearly for Phase Retrieval, Matrix Completion, and Blind Deconvolution. *Foundations of Computational Mathematics*, 20(3):451–632, June 2020.

A Used distributions

The main distributions that we use throughout the text are

- the Gaussian distribution with mean $\mu \in \mathbb{R}$ and precision $\beta > 0$ (the inverse of variance)

$$\mathcal{N}(x|\mu, \beta^{-1}) = \sqrt{\frac{\beta}{2\pi}} e^{-\frac{\beta}{2}(x-\mu)^2};$$

- the multivariate Gaussian distribution with mean $\mu \in \mathbb{R}^n$ and positive definite precision matrix B

$$\mathcal{N}(x|\mu, B^{-1}) = \sqrt{\frac{\det B}{(2\pi)^n}} e^{-\frac{1}{2}(x-\mu)^T B (x-\mu)};$$

- the Gamma distribution with shape $a > 0$ and rate $b > 0$ parameters

$$\mathcal{G}(x|a, b) = \frac{b^a x^{a-1} e^{-bx}}{\Gamma(a)}.$$

All of them belong to the exponential family of distributions because their densities can be expressed as

$$\mathcal{N}(x|\mu, \beta^{-1}) = \exp \left\{ \begin{bmatrix} \beta\mu \\ -\frac{\beta}{2} \end{bmatrix}^T \begin{bmatrix} x \\ x^2 \end{bmatrix} + \frac{1}{2}(\log \beta - \beta\mu^2 - \log 2\pi) \right\},$$

$$\mathcal{G}(x|a, b) = \exp \left\{ \begin{bmatrix} -b \\ a-1 \end{bmatrix}^T \begin{bmatrix} x \\ \log x \end{bmatrix} + (a \log b - \log \Gamma(a)) \right\},$$

$$\mathcal{N}(x|\mu, B^{-1}) = \exp \left\{ \begin{bmatrix} B\mu \\ \text{col}(B) \end{bmatrix}^T \begin{bmatrix} x \\ \text{col}(xx^T) \end{bmatrix} + \frac{1}{2}(\log \det B - \mu^T B \mu - n \log 2\pi) \right\}.$$

Consider a probabilistic model, where a Gamma prior $\mathcal{G}(\beta|a, b)$ is put on the precision of a Gaussian distribution $\mathcal{N}(x|\mu, \beta^{-1})$. This is a simple example of what is known as a conjugate-exponential model: the parameter β that establishes the link between the two distributions enters both of them as $[\beta \quad \log \beta]^T$. If we marginalize it out, we get the Student's t -distribution

$$\text{St} \left(x \middle| \mu, \frac{a}{b}, 2a \right) = \int_0^\infty \mathcal{N}(x|\mu, \beta^{-1}) \mathcal{G}(\beta|a, b) d\beta = \frac{\Gamma(a+1/2)}{\Gamma(a)} \sqrt{\frac{1}{2\pi b}} \left[1 + \frac{(x-\mu)^2}{2b} \right]^{\frac{1}{2}-a}$$

with mean μ and variance $b/(a-1)$.

B Optimal factorized variational distributions

B.1 General form

Recall that in variational Bayesian inference our goal is to minimize the Kullback–Leibler divergence between the variational posterior $q(\Theta)$ and the real posterior $p(\Theta|Y_\Omega)$, or, equivalently, to minimize

$$F(q) = \int q(\Theta) \log \frac{q(\Theta)}{p(Y_\Omega, \Theta)} d\Theta \rightarrow \min_{q(\Theta)}.$$

Let us look for $q(\Theta)$ in a factorized form

$$q(\Theta) = \prod_i q(\theta_i)$$

and substitute it into the minimization problem:

$$\begin{aligned} F(q) &= \int q(\Theta) \log q(\Theta) d\Theta - \int q(\Theta) \log p(Y_\Omega, \Theta) d\Theta \\ &= \sum_j \int q(\theta_j) \log q(\theta_j) d\theta_j - \int q(\Theta) \log p(Y_\Omega, \Theta) d\Theta \\ &= \sum_j \int q(\theta_j) \log q(\theta_j) d\theta_j - \int q(\theta_i) \underbrace{\left\{ \int \prod_{j \neq i} q(\theta_j) \log p(Y_\Omega, \Theta) \prod_{j \neq i} d\theta_j \right\}}_{\log q^*(\theta_i) + \text{const}} d\theta_i \\ &= \sum_{j \neq i} \int q(\theta_j) \log q(\theta_j) d\theta_j - \int q(\theta_i) \log \frac{q^*(\theta_i)}{q(\theta_i)} d\theta_i + \text{const} \\ &= \sum_{j \neq i} \int q(\theta_j) \log q(\theta_j) d\theta_j + \mathcal{KL}[q(\theta_i) \parallel q^*(\theta_i)] + \text{const}. \end{aligned}$$

Since the Kullback–Leibler divergence is non-negative and equals to zero if and only if the two distributions coincide almost everywhere, we must choose $q(\theta_i) = q^*(\theta_i)$ to minimize $F(q)$ if all the remaining $q(\theta_j)$ are fixed.

B.2 Matrix case

To compute $q^*(\theta_i)$ according to

$$\log q^*(\theta_i) = \mathbb{E}_{\sim \theta_i} \{\log p(Y_\Omega, \Theta)\} + \text{const},$$

we basically need to expand $\log p(Y_\Omega, \Theta)$ and collect the relevant terms. This is where the exponential conjugacy of our model comes in handy.

B.2.1 Factor matrices U and V

Let us begin with the factor matrix U . Recall that we write $\bar{u} \in \mathbb{R}^{m_1 k}$ and $\bar{v} \in \mathbb{R}^{m_2 k}$ for the vectorizations of U and V obtained by stacking their columns as

$$\bar{u} = [u_{11} \ \dots \ u_{m_1 1} \ u_{12} \ \dots \ u_{m_1 k}]^T, \quad \bar{v} = [v_{11} \ \dots \ v_{m_2 1} \ v_{12} \ \dots \ v_{m_2 k}]^T.$$

For brevity, we will also use the following notation:

$$g_{i_1}^T U V^T h_{i_2} = \bar{u}^T (I_k \otimes g_{i_1} h_{i_2}^T) \bar{v} = \bar{u}^T \bar{\varphi}_{i_1 i_2}.$$

Then we have

$$\begin{aligned}
\log p(Y_\Omega, \Theta) &= \sum_{\Omega} \log p(y_{i_1 i_2} | U, V, \tau) + \sum_{j_1=1}^{m_1} \log p(u_{j_1} | \Lambda) + \dots \\
&= \sum_{\Omega} \left\{ \tau y_{i_1 i_2} \bar{u}^T \bar{\varphi}_{i_1 i_2} - \frac{\tau}{2} \bar{u}^T \bar{\varphi}_{i_1 i_2} \bar{\varphi}_{i_1 i_2}^T \bar{u} \right\} + \sum_{j_1=1}^{m_1} \left\{ -\frac{1}{2} u_{j_1}^T \Lambda u_{j_1} \right\} + \dots \\
&= \sum_{\Omega} \left\{ \tau y_{i_1 i_2} \bar{u}^T \bar{\varphi}_{i_1 i_2} - \frac{\tau}{2} \bar{u}^T \bar{\varphi}_{i_1 i_2} \bar{\varphi}_{i_1 i_2}^T \bar{u} \right\} - \frac{1}{2} \bar{u}^T (\Lambda \otimes I_{m_1}) \bar{u} + \dots \\
&= -\frac{1}{2} \bar{u}^T \left(\Lambda \otimes I_{m_1} + \tau \sum_{\Omega} \bar{\varphi}_{i_1 i_2} \bar{\varphi}_{i_1 i_2}^T \right) \bar{u} + \bar{u}^T \left(\tau \sum_{\Omega} y_{i_1 i_2} \bar{\varphi}_{i_1 i_2} \right) + \dots
\end{aligned}$$

By comparing this formula with the multivariate Gaussian distribution, we readily see that $q^*(U)$ is a Gaussian distribution

$$q^*(U) = \mathcal{N}(\bar{u} | \mu_{\bar{u}}, A_{\bar{u}})$$

with covariance

$$\begin{aligned}
A_{\bar{u}} &= \left[\mathbb{E} \left\{ \Lambda \otimes I_{m_1} + \tau \sum_{\Omega} \bar{\varphi}_{i_1 i_2} \bar{\varphi}_{i_1 i_2}^T \right\} \right]^{-1} \\
&= \left[\mathbb{E} \{ \Lambda \} \otimes I_{m_1} + \mathbb{E} \{ \tau \} \sum_{\Omega} \mathbb{E} \{ \bar{\varphi}_{i_1 i_2} \bar{\varphi}_{i_1 i_2}^T \} \right]^{-1} \\
&= \left[\mathbb{E} \{ \Lambda \} \otimes I_{m_1} + \mathbb{E} \{ \tau \} \sum_{\Omega} (I_k \otimes g_{i_1} h_{i_2}^T) \mathbb{E} \{ \bar{v} \bar{v}^T \} (I_k \otimes h_{i_2} g_{i_1}^T) \right]^{-1} \\
&= \left[\mathbb{E} \{ \Lambda \} \otimes I_{m_1} + \mathbb{E} \{ \tau \} \sum_{\Omega} (I_k \otimes h_{i_2}^T) \mathbb{E} \{ \bar{v} \bar{v}^T \} (I_k \otimes h_{i_2}) \otimes g_{i_1} g_{i_1}^T \right]^{-1}
\end{aligned}$$

and mean

$$\begin{aligned}
\mu_{\bar{u}} &= A_{\bar{u}} \mathbb{E} \left\{ \tau \sum_{\Omega} y_{i_1 i_2} \bar{\varphi}_{i_1 i_2} \right\} \\
&= \mathbb{E} \{ \tau \} A_{\bar{u}} \sum_{\Omega} y_{i_1 i_2} (I_k \otimes g_{i_1} h_{i_2}^T) \mathbb{E} \{ \bar{v} \} \\
&= \mathbb{E} \{ \tau \} A_{\bar{u}} \sum_{\Omega} y_{i_1 i_2} (I_k \otimes h_{i_2}^T) \mathbb{E} \{ \bar{v} \} \otimes g_{i_1}.
\end{aligned}$$

We used the factorized form of $q(\Theta)$ in decoupling the expectations. The second factor matrix V is dealt with in complete analogy.

B.2.2 Precision matrix Λ

For the precision matrix, we keep track of different terms in the expansion:

$$\begin{aligned}
\log p(Y_\Omega, \Theta) &= \sum_{i_1=1}^{m_1} \log p(u_{i_1} | \Lambda) + \sum_{i_2=1}^{m_2} \log p(v_{i_2} | \Lambda) + \sum_{j=1}^k \log p(\lambda_j) + \dots \\
&= \sum_{i_1=1}^{m_1} \left\{ -\frac{1}{2} u_{i_1}^T \Lambda u_{i_1} + \frac{1}{2} \sum_{j=1}^k \log \lambda_j \right\} + \sum_{i_2=1}^{m_2} \left\{ -\frac{1}{2} v_{i_2}^T \Lambda v_{i_2} + \frac{1}{2} \sum_{j=1}^k \log \lambda_j \right\} \\
&\quad + \sum_{j=1}^k \{ -b_j \lambda_j + (a_j - 1) \log \lambda_j \} + \dots \\
&= \sum_{j=1}^k \left\{ \lambda_j \left(-b_j - \frac{1}{2} \sum_{i_1=1}^{m_1} u_{i_1 j}^2 - \frac{1}{2} \sum_{i_2=1}^{m_2} v_{i_2 j}^2 \right) + \log \lambda_j \left(a_j - 1 + \frac{m_1}{2} + \frac{m_2}{2} \right) \right\} + \dots \\
&= \sum_{j=1}^k \left\{ \lambda_j \left(-b_j - \frac{1}{2} (U^T U)_{jj} - \frac{1}{2} (V^T V)_{jj} \right) + \log \lambda_j \left(a_j - 1 + \frac{m_1}{2} + \frac{m_2}{2} \right) \right\} + \dots
\end{aligned}$$

It follows, given the expression of the Gamma distribution as an element of the exponential family, that

$$q^*(\Lambda) = \prod_{j=1}^k \mathcal{G}(\lambda_j | c_j, d_j)$$

with

$$c_j = a_j + \frac{m_1 + m_2}{2}, \quad d_j = b_j + \frac{1}{2} \mathbb{E}\{U^T U\}_{jj} + \frac{1}{2} \mathbb{E}\{V^T V\}_{jj}, \quad j = 1, \dots, k.$$

B.2.3 Noise precision τ

In the same vein, we get

$$\begin{aligned}
\log p(Y_\Omega, \Theta) &= \sum_{\Omega} \log p(y_{i_1 i_2} | U, V, \tau) + \log p(\tau) + \dots \\
&= \sum_{\Omega} \left\{ -\frac{\tau}{2} (y_{i_1 i_2} - g_{i_1}^T U V^T h_{i_2})^2 + \frac{1}{2} \log \tau \right\} + \{ -b_0 \tau + (a_0 - 1) \log \tau \} + \dots \\
&= \tau \left(-b_0 - \frac{1}{2} \sum_{\Omega} (y_{i_1 i_2} - g_{i_1}^T U V^T h_{i_2})^2 \right) + \log \tau \left(a_0 - 1 + \frac{|\Omega|}{2} \right) + \dots
\end{aligned}$$

Hence

$$q^*(\tau) = \mathcal{G}(\tau | c_0, d_0)$$

with

$$c_0 = a_0 + \frac{|\Omega|}{2}, \quad d_0 = b_0 + \frac{1}{2} \mathbb{E} \left\{ \|Y_\Omega - \mathcal{P}_\Omega(GUV^T H^T)\|_F^2 \right\}.$$

B.3 Tensor case

B.3.1 Canonical factors U_l

For tensors, it is sufficient to note that

$$\langle U_1^T g_{1,i_1}, \dots, U_d^T g_{d,i_d} \rangle = \bar{u}_l^T (I_k \otimes g_{l,i_l}) \bigcirc_{s \neq l} (I_k \otimes g_{s,i_s}^T) \bar{u}_s = \bar{u}_l^T \bar{\varphi}_{i_1 \dots i_d}.$$

We then immediately arrive at

$$\begin{aligned}\log p(\mathbf{Y}_\Omega, \Theta) &= \sum_{\Omega} \log p(y_{i_1 \dots i_d} | U_1, \dots, U_d, \tau) + \sum_{j_l=1}^{m_l} \log p(u_{l,j_l} | \Lambda) + \dots \\ &= -\frac{1}{2} \bar{u}_l^T \left(\Lambda \otimes I_{m_l} + \tau \sum_{\Omega} \bar{\varphi}_{i_1 \dots i_d} \bar{\varphi}_{i_1 \dots i_d}^T \right) \bar{u}_l + \bar{u}_l^T \left(\tau \sum_{\Omega} y_{i_1 \dots i_d} \bar{\varphi}_{i_1 \dots i_d} \right) + \dots\end{aligned}$$

and recognize a Gaussian distribution. On taking the expectation $\mathbb{E}_{\sim U_l}$, we get the covariance matrix A_l of the optimal posterior distribution

$$\begin{aligned}A_l &= \left[\mathbb{E} \left\{ \Lambda \otimes I_{m_l} + \tau \sum_{\Omega} \bar{\varphi}_{i_1 \dots i_d} \bar{\varphi}_{i_1 \dots i_d}^T \right\} \right]^{-1} \\ &= \left[\mathbb{E}\{\Lambda\} \otimes I_{m_l} + \mathbb{E}\{\tau\} \sum_{\Omega} \mathbb{E}\{\bar{\varphi}_{i_1 \dots i_d} \bar{\varphi}_{i_1 \dots i_d}^T\} \right]^{-1} \\ &= \left[\mathbb{E}\{\Lambda\} \otimes I_{m_l} + \mathbb{E}\{\tau\} \sum_{\Omega} (I_k \otimes g_{l,i_l}) \mathbb{E} \left\{ \bigodot_{s \neq l} (I_k \otimes g_{s,i_s}^T) \bar{u}_s \bar{u}_s^T (I_k \otimes g_{s,i_s}) \right\} (I_k \otimes g_{l,i_l}^T) \right]^{-1} \\ &= \left[\mathbb{E}\{\Lambda\} \otimes I_{m_l} + \mathbb{E}\{\tau\} \sum_{\Omega} (I_k \otimes g_{l,i_l}) \left(\bigodot_{s \neq l} (I_k \otimes g_{s,i_s}^T) \mathbb{E}\{\bar{u}_s \bar{u}_s^T\} (I_k \otimes g_{s,i_s}) \right) (I_k \otimes g_{l,i_l}^T) \right]^{-1} \\ &= \left[\mathbb{E}\{\Lambda\} \otimes I_{m_l} + \mathbb{E}\{\tau\} \sum_{\Omega} \left(\bigodot_{s \neq l} (I_k \otimes g_{s,i_s}^T) \mathbb{E}\{\bar{u}_s \bar{u}_s^T\} (I_k \otimes g_{s,i_s}) \right) \otimes g_{l,i_l} g_{l,i_l}^T \right]^{-1}\end{aligned}$$

and the corresponding mean

$$\begin{aligned}\mu_l &= A_l \mathbb{E} \left\{ \tau \sum_{\Omega} y_{i_1 \dots i_d} \bar{\varphi}_{i_1 \dots i_d} \right\} \\ &= \mathbb{E}\{\tau\} A_l \sum_{\Omega} y_{i_1 \dots i_d} (I_k \otimes g_{l,i_l}^T) \mathbb{E} \left\{ \bigodot_{s \neq l} U_s^T g_{s,i_s} \right\} \\ &= \mathbb{E}\{\tau\} A_l \sum_{\Omega} y_{i_1 \dots i_d} (I_k \otimes g_{l,i_l}^T) \left(\bigodot_{s \neq l} \mathbb{E}\{U_s^T\} g_{s,i_s} \right) \\ &= \mathbb{E}\{\tau\} A_l \sum_{\Omega} y_{i_1 \dots i_d} \left(\bigodot_{s \neq l} \mathbb{E}\{U_s^T\} g_{s,i_s} \right) \otimes g_{l,i_l}.\end{aligned}$$

In the derivation, we used the mixed-product property of the Hadamard product

$$\left[\bigodot_{s \neq l} (I_k \otimes g_{s,i_s}^T) \bar{u}_s \right] \left[\bigodot_{s \neq l} (I_k \otimes g_{s,i_s}^T) \bar{u}_s \right]^T = \bigodot_{s \neq l} (I_k \otimes g_{s,i_s}^T) \bar{u}_s \bar{u}_s^T (I_k \otimes g_{s,i_s}),$$

and the factorized form of $q(\Theta)$ allowed us to compute its expectation.

B.3.2 Precision matrix Λ

In analogy with the matrix case, we have

$$\begin{aligned}
\log p(\mathbf{Y}_\Omega, \Theta) &= \sum_{l=1}^d \sum_{i_l=1}^{m_l} \log p(u_{l,i_l} | \Lambda) + \sum_{j=1}^k \log p(\lambda_j) + \dots \\
&= \sum_{l=1}^d \sum_{i_l=1}^{m_l} \left\{ -\frac{1}{2} u_{l,i_l}^T \Lambda u_{l,i_l} + \frac{1}{2} \sum_{j=1}^k \log \lambda_j \right\} + \sum_{j=1}^k \{ -b_j \lambda_j + (a_j - 1) \log \lambda_j \} + \dots \\
&= \sum_{j=1}^k \left\{ \lambda_j \left(-b_j - \frac{1}{2} \sum_{l=1}^d \sum_{i_l=1}^{m_l} u_{l,i_l}^2 \right) + \log \lambda_j \left(a_j - 1 + \frac{1}{2} \sum_{l=1}^d m_l \right) \right\} + \dots
\end{aligned}$$

and, as a result,

$$q^*(\Lambda) = \prod_{j=1}^k \mathcal{G}(\lambda_j | c_j, d_j)$$

with

$$c_j = a_j + \frac{1}{2} \sum_{l=1}^d m_l, \quad d_j = b_j + \frac{1}{2} \sum_{l=1}^d \mathbb{E}\{U_l^T U_l\}_{jj}, \quad j = 1, \dots, k.$$

B.3.3 Noise precision τ

We repeat the computation yet again to get

$$\begin{aligned}
\log p(\mathbf{Y}_\Omega, \Theta) &= \sum_{\Omega} \log p(y_{i_1 \dots i_d} | U_1, \dots, U_d, \tau) + \log p(\tau) + \dots \\
&= \sum_{\Omega} \left\{ -\frac{\tau}{2} \left(y_{i_1 \dots i_d} - \langle U_1^T g_{1,i_1}, \dots, U_d^T g_{d,i_d} \rangle \right)^2 + \frac{1}{2} \log \tau \right\} + \{ -b_0 \tau + (a_0 - 1) \log \tau \} + \dots \\
&= \tau \left(-b_0 - \frac{1}{2} \sum_{\Omega} \left(y_{i_1 \dots i_d} - \langle U_1^T g_{1,i_1}, \dots, U_d^T g_{d,i_d} \rangle \right)^2 \right) + \log \tau \left(a_0 - 1 + \frac{|\Omega|}{2} \right) + \dots
\end{aligned}$$

Consequently,

$$q^*(\tau) = \mathcal{G}(\tau | c_0, d_0)$$

with

$$c_0 = a_0 + \frac{|\Omega|}{2}, \quad d_0 = b_0 + \frac{1}{2} \mathbb{E} \left\{ \|\mathbf{Y}_\Omega - \mathcal{P}_\Omega[G_1 U_1, \dots, G_d U_d]\|_F^2 \right\}.$$

B.4 Computing the expectations

To get explicit formulas for the optimal distributions, we need to take the expectations. The only non-trivial ones are related to the rate parameters d_j and d_0 of precision matrix Λ and noise precision τ , respectively.

First, note that $(U_l^T U_l)_{jj}$ is the squared Euclidean norm of the j -th column of U_l or, in other words, of the j -th subvector of \bar{u}_l of length m_l . The outer product of this subvector with itself is exactly the j -th diagonal block of $\bar{u}_l \bar{u}_l^T$ of size $m_l \times m_l$, and its components squared lie on the diagonal of the block; hence the trace.

Second, we use the following property of the multi-linear product

$$\langle U_1^T g_{1,i_1}, \dots, U_d^T g_{d,i_d} \rangle^2 = \langle U_1^T g_{1,i_1} g_{1,i_1}^T U_1, \dots, U_d^T g_{d,i_d} g_{d,i_d}^T U_d \rangle$$

together with $U_l^T g_{l,i_l} = (I_{m_l} \otimes g_{l,i_l}^T) \bar{u}_l$. The factorized form of $q(\Theta)$ allows us to compute the expectations individually for each matrix in the multi-linear product.

C Distribution of predicted values

Let us show how the Student's t -distribution arises when we try to predict the unknown elements of a matrix/tensor based on the given ones \mathbf{Y}_Ω . We have

$$\begin{aligned} p(y_{i_1 \dots i_d} | \mathbf{Y}_\Omega) &= \int p(y_{i_1 \dots i_d} | U_1, \dots, U_d, \tau) p(U_1, \dots, U_d, \Lambda, \tau | \mathbf{Y}_\Omega) \prod_{l=1}^d dU_l d\Lambda d\tau \\ &\approx \int p(y_{i_1 \dots i_d} | U_1, \dots, U_d, \tau) \prod_{l=1}^d q^*(U_l) q^*(\tau) \prod_{l=1}^d dU_l d\tau. \end{aligned}$$

If one puts a Gaussian prior over the mean of another Gaussian random variable and marginalizes it out, the resulting distribution will be Gaussian as well, whose variance is the sum of two variances:

$$\int \mathcal{N}(x | \mu, \tau^{-1}) \mathcal{N}(\mu | m, s^{-1}) d\mu = \mathcal{N}(x | m, \tau^{-1} + s^{-1}).$$

A similar result can be obtained with the Sherman–Morrison formula for

$$\int \mathcal{N}(x | u^T v, \tau^{-1}) \mathcal{N}(u | \mu, A) du = \mathcal{N}(y | \mu^T v, \tau^{-1} + v^T A v).$$

It then follows that we can marginalize out the contribution of U_1 :

$$\begin{aligned} p(y_{i_1 \dots i_d} | \mathbf{Y}_\Omega) &\approx \int \mathcal{N}(y_{i_1 \dots i_d} | \langle U_1^T g_{1,i_1}, \dots, U_d^T g_{d,i_d} \rangle, \tau^{-1}) \prod_{l=1}^d \mathcal{N}(\bar{u}_l | \mu_l, A_l) \mathcal{G}(\tau | c_0, d_0) \prod_{l=1}^d dU_l d\tau \\ &= \int \mathcal{N}(y_{i_1 \dots i_d} | \langle M_1^T g_{1,i_1}, \dots, U_d^T g_{d,i_d} \rangle, \tau^{-1} + \tilde{\eta}_1) \prod_{l=2}^d \mathcal{N}(\bar{u}_l | \mu_l, A_l) \mathcal{G}(\tau | c_0, d_0) \prod_{l=2}^d dU_l d\tau, \end{aligned}$$

where

$$\tilde{\eta}_1 = \left(\bigodot_{s \neq 1} U_s^T g_{s,i_s} \right)^T (I_k \otimes g_{1,i_1}^T) A_1 (I_k \otimes g_{1,i_1}) \left(\bigodot_{s \neq 1} U_s^T g_{s,i_s} \right).$$

Now, we cannot apply directly the same idea since both mean and variance depend on U_2 . So, in order to proceed, we have to make an approximation by replacing all U_l with their mean values:

$$\tilde{\eta}_1 \approx \eta_1 = \left(\bigodot_{s \neq 1} M_s^T g_{s,i_s} \right)^T (I_k \otimes g_{1,i_1}^T) A_1 (I_k \otimes g_{1,i_1}) \left(\bigodot_{s \neq 1} M_s^T g_{s,i_s} \right).$$

Repeating this for l from 2 through d , we arrive at

$$p(y_{i_1 \dots i_d} | \mathbf{Y}_\Omega) \approx \int \mathcal{N}(y_{i_1 \dots i_d} | \langle M_1^T g_{1,i_1}, \dots, M_d^T g_{d,i_d} \rangle, \tau^{-1} + \eta) \mathcal{G}(\tau | c_0, d_0) d\tau$$

with

$$\eta = \sum_{l=1}^d \eta_l = \sum_{l=1}^d \left(\bigodot_{s \neq l} M_s^T g_{s,i_s} \right)^T (I_k \otimes g_{l,i_l}^T) A_l (I_k \otimes g_{l,i_l}) \left(\bigodot_{s \neq l} M_s^T g_{s,i_s} \right).$$

The integral is exactly the Student's t -distribution

$$\text{St}(y_{i_1 \dots i_d} | \langle M_1^T g_{1,i_1}, \dots, M_d^T g_{d,i_d} \rangle, (d_0/c_0 + \eta)^{-1}, 2c_0).$$

D Additional numerical experiments with synthetic data

Phase plots can be built for fixed n and varying r too. In Fig 8 we compare the phase transitions of matrices and 3-dimensional tensors without side information obtained with FBCP (we made $N_{trial} = 5$ trials with $N_{ic} = 2$ different initial conditions, making $N_{iter} = 100$ iterations for $d = 2$ and $N_{iter} = 150$ iterations for $d = 3$). Fig. 9 shows the regularization effects of side information for $d = 3$, $n = 50$, $m = 30$: the phase transition curve becomes lower, and the successes become more consistent above the curve.

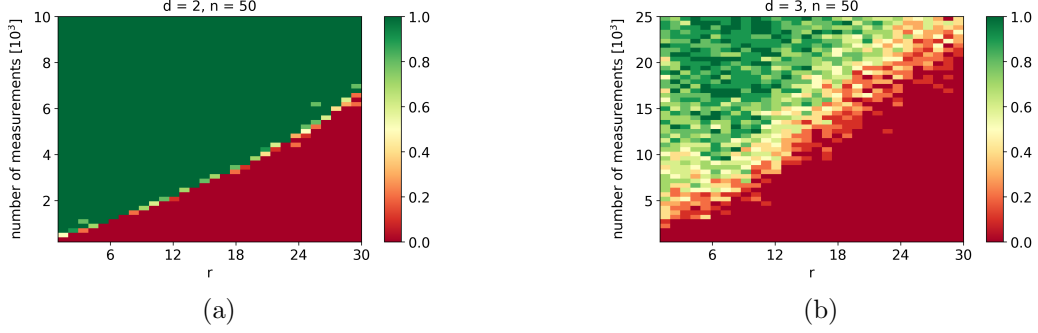


Figure 8: Phase plots for noiseless CP completion with size $n = 50$, varying rank r , perfect rank prediction $k = r$, and no side information for different orders of the tensor: $d = 2$ (a) and $d = 3$ (b).

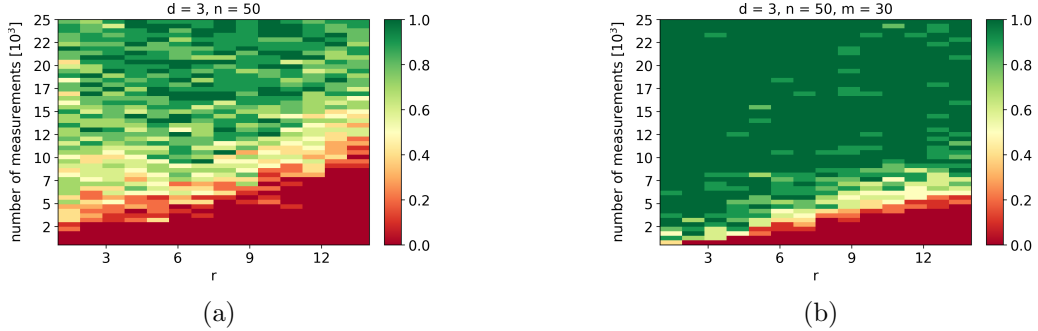


Figure 9: Phase plots for noiseless 3-dimensional CP completion with size $n = 50$, varying rank r , and perfect rank prediction $k = r$: FBCP (a) and FBCP-SI with $m = 30$ (b).

Next, we compare the convergence rates of FBCP and FBCP-SI on the test samples $\Omega_{test}^{(t)}$ for rank-3 CP tensors of size $400 \times 400 \times 400$. In both cases, there are two phases of convergence: a plateau of nearly constant error followed by its linear decay. The more elements of the tensor are known, the shorter the plateau, and side information decreases its length even further. However, the length also depends on the initialization; for instance, we observe that the iterations can converge with one random initialization but not with the other. The rate of linear convergence differs for FBCP and FBCP-SI: the former takes 5-10 iterations to drop the relative error below 10^{-6} while the latter requires 30-40 iterations (for $m = 30$).

Another important aspect is how FBCP-SI performs in the presence of noise. In Fig. 12 we present the results of experiments with random rank-3 CP tensors of sizes $100 \times 100 \times 100$ for different values of $|\Omega|$ and m (the rank is assumed to be known). For varying levels of noise, we plot the RMSE on the test samples after $N_{iter} = 100$ iterations, averaged over $N_{trial} = 20$ trials with $N_{ic} = 1$. The results show that the error is proportional to the standard deviation

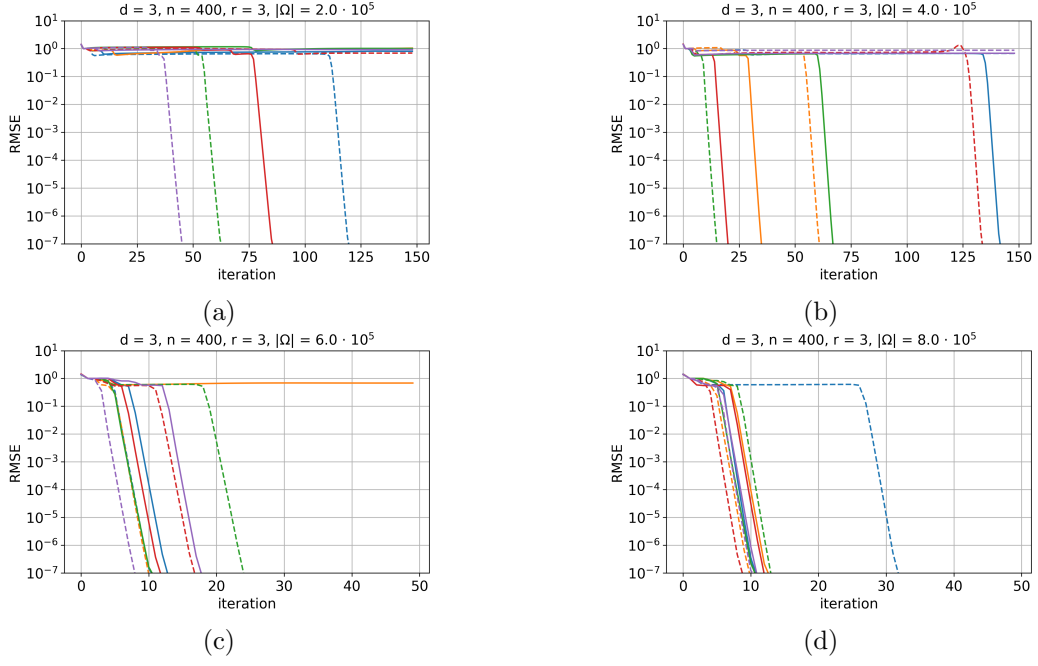


Figure 10: Convergence curves for noiseless 3-dimensional CP completion with size $n = 400$, rank $r = 3$, perfect rank prediction $k = 3$, no side information, and different numbers of samples: $|\Omega| = 2 \cdot 10^5$ (a), $|\Omega| = 4 \cdot 10^5$ (b), $|\Omega| = 6 \cdot 10^5$ (c), and $|\Omega| = 8 \cdot 10^5$ (d). Solid and dashed lines of the same color correspond to 2 different initial conditions.

of additive white Gaussian noise and that smaller m (i.e. more informative side information) leads to lower errors. Notably, the signals are recovered from noise as high as -10dB.

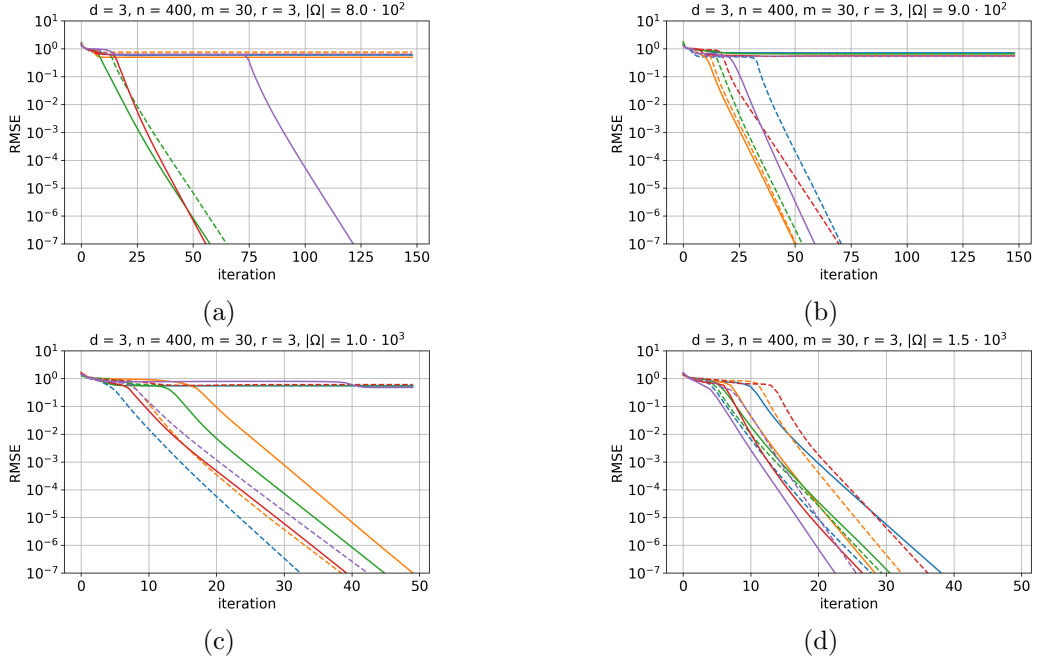


Figure 11: Convergence curves for noiseless 3-dimensional CP completion with size $n = 400$, rank $r = 3$, perfect rank prediction $k = 3$, side information size $m = 30$, and different numbers of samples: $|\Omega| = 8 \cdot 10^2$ (a), $|\Omega| = 9 \cdot 10^2$ (b), $|\Omega| = 1 \cdot 10^3$ (c), and $|\Omega| = 1.5 \cdot 10^3$ (d). Solid and dashed lines of the same color correspond to 2 different initial conditions.

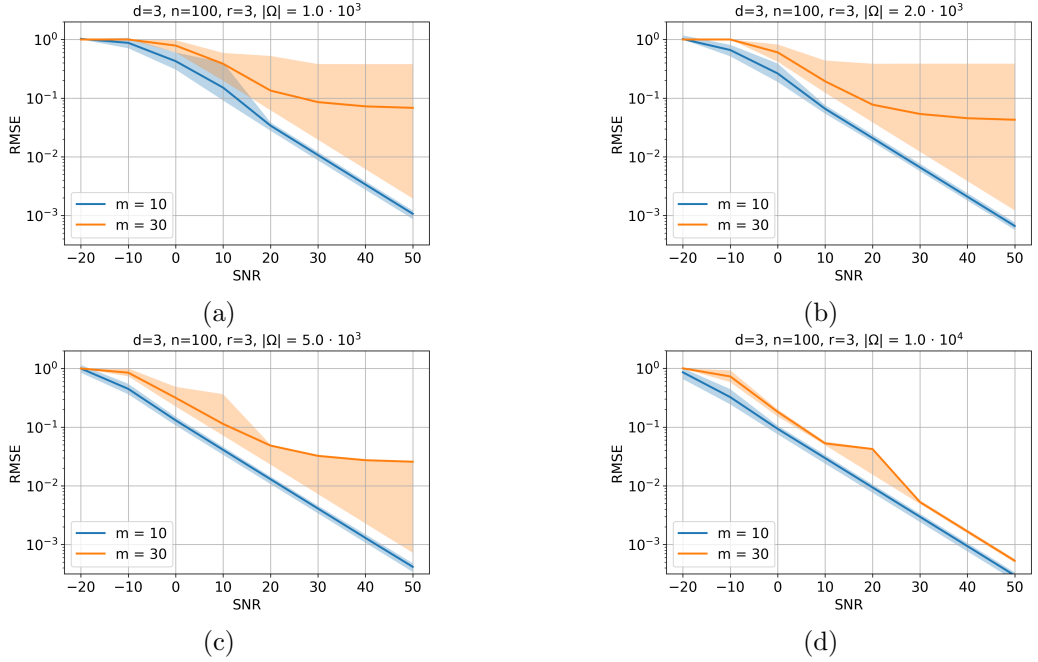


Figure 12: Attainable RMSE for 3-dimensional CP completion with size $n = 100$, rank $r = 3$, perfect rank prediction $k = 3$, varying levels of noise and different numbers of samples: $|\Omega| = 1 \cdot 10^3$ (a), $|\Omega| = 2 \cdot 10^3$ (b), $|\Omega| = 5 \cdot 10^3$ (c), and $|\Omega| = 1 \cdot 10^4$ (d). The curves show the averaged RMSE together with the 5th and 95th percentiles for side information sizes $m = 10$ and $m = 30$.